ENTANGLED PHOTONS STUDY BASED ON MACH ZEHNDER INTERFEROMETER

SUEBTARKUL SUCHAT

A THESIS SUBMITTED IN FULFILLMENT

OF THE REQUIREMENT FOR THE DEGREE OF

DOCTOR OF PHILOSOPHY IN APPLIED PHYSICS

SCHOOL OF GRADUATE STUDIES

KING MONGKUT'S INSTITUTE OF TECHNOLOGY LADKRABANG

2007

KMITL-2007-SC-D-030-104

หัวข้อวิทยานิพนธ์	การศึกษาโฟตอนเอนแทงเกิลโดยการใช้แมคเซห์นเดอร์อินเตอร์ฟีรอมิเตอร์
นักศึกษา	นายสืบตระกูล สุชาติ
รหัสประจำตัว	43065902
ปริญญา	ปรัชญาดุษฎีบัณฑิต
สาขาวิชา	ฟิสิกส์ประยุกต์
พ.ศ.	2550
อาจารย์ที่ปรึกษาวิทยานิพนธ์	รศ.ดร. ปรีชา ยุพาพิน

บทคัดย่อ

ในวิทยานิพนธ์เป็นมีการศึกษาโฟตอนเอนแทงเกิลโดยการใช้แมคเซห์นเดอร์อินเตอร์ฟีรอมิเตอร์ โดยโฟตอนที่สร้างขึ้นและแอนแทงเกิล นี้ได้จากการใช้แสงโพลาไรซ์ต่อเนื่องส่งผ่านเข้าไปในผลึกลิเทียมไนโอเบต ($LiNbO_3$) ซึ่งอยู่ในแขนข้างหนึ่งแมคเซห์นเดอร์อินเตอร์ฟีรอมิเตอร์ และทำการมอดูเลตแสงด้วยการใส่สัญญาณความถี่ผ่านทางขั้วซึ่งต่ออยู่กับผลึกลิเทียมไนโอเบต และยังมีการใช้เทคนิคใหม่ในการสร้างคู่เอนแทงเกิลโฟตอนด้วยการใช้เส้นใยแก้วนำแสงทั้งหมด ซึ่งในระบบจะใช้แมคเซห์นเดอร์อินเตอร์ฟีรอมิเตอร์ ร่วมกับวงแหวนของการสั่นพ้องที่ใช้เส้นใยแก้วนำแสงทั้งหมด ซึ่งข้อดีของระบบนี้เป็นระบบที่ง่ายในการสร้างและไม่ต้องมีส่วนของการปั้ม หรือส่วนประกอบที่มีขนาดใหญ่ เมื่อแสงโพลาไรซ์ซึ่งเป็นขบวนพัลส์ส่งผ่านเข้าไปในแมคเซห์นเดอร์อินเตอร์ฟีรอมิเตอร์ ที่มีความยาวของแขนสองข้างไม่เท่ากัน ทำให้พัลส์ที่ได้จากแมคเซห์นเดอร์อินเตอร์ฟีรอมิเตอร์ ออกมานั้นเดินทางช้ากว่ากัน จากนั้นส่งผ่านเข้าไปยังวงแหวนของการสั่นพ้องที่ใช้เส้นใยแก้วซึ่งมีตัวควบคุมแสงโพลาไรซ์อยู่ พัลส์จะหมุนวนในวงแหวนของการสั่นพ้องแบบไม่เป็นเชิงเส้นซึ่งจะเกิดการซ้อนกันของพัลส์เหล่านั้นขึ้น และส่งผ่านออกมา หลังจากนั้น ได้ทำการตรวจวัดคุณลักษณะของการเป็นเอนแทงเกิลโดยการใช้โฟโตไดโอดชนิดอาวาลันช์ โดยผลที่ได้ออกมานั้นได้ผลเป็นอย่างดีซึ่งสามารถนำไปใช้งานได้ต่อไป

Thesis Title	Entangled Photons Study Based on Mach Zehnder Interferometer
Student	Mr. Suebtarkul Suchat
Student ID.	43065902
Degree	Doctor of Philosophy
Program	Applied Physics
Year	2007
Thesis Advisor	Associate Professor Dr. Preecha Yupapin

ABSTRACT

In this thesis, the study of the entanglement of photons based on a Mach Zehnder interferometer is described. The entangled photons are generated when polarized light propagates into one arm of MZI, which is pumped via a $LiNbO_3$. The principle of the technique is that a CW laser output is launched into the classical Mach-Zehnder Interferometer then modulated via a $LiNbO_3$. A new technique of the entangled photon pair generation using an all fiber optic scheme is also investigated. The proposed system consists of a fiber optic Mach-Zhender Interferometer (MZI) incorporating a fiber optic ring resonator. The advantage of such a system is that it requires a simple arrangement without any optical pumping part or bulky optical components. Polarized light pulse trains are launched randomly into a MZI, one part of light is delayed in the longer path. The output pulses from both arms of the MZI enter a fiber optic ring resonator. A polarization controller controls polarization states of light pulses while they circulate in the ring resonator. The superposition of the nonlinear light pulses in a fiber optic ring resonator randomly occurred. These forms are seen on the avalanche photo detectors. The results are in good agreement with the theoretical prediction.

ACKNOWLEDGMENTS

Years of extensive research and intense studies have finally culminated to form the basis of my thesis, which represents the efforts and hard work committed to furthering my education. Completing this thesis would not have been possible without the contributions of many people. I am greatly indebted to Assoc.Prof.Dr.Preecha Yupapin, my advisor, for their helpful supervision during the preparation and completion of this thesis. I would like to thank Assist.Prof.Dr.Surasak Chiangga for helping in give me advice to approve my thesis. I would like to acknowledge to the National Science and Technology Development Agency (NSTDA) and Department of Physics, Faculty of Science and Technology, Thammasat University, Thailand for partially financial support of his study.

Finally, I would like to express my deep gratitude to my family and friends for their encouragement throughout my graduate studies.

Suebtarkul Suchat

TABLE OF CONTENTS

TABLE OF CONTENTS (cont.)

LIST OF FIGURES

Figures Page

CHAPTER 1

INTRODUCTION

1.1 Motivation

Quantum entanglement is a physical resource, like energy, associated with the peculiar nonclassical correlations that are possible between separated quantum systems. In effect, the very possibility of considering a particle or system as possessing objective properties depends on its entanglement with another particle or system. Quantum entanglement has been widely studied and investigated during the 1990s. The Austrian-born Erwin Schrodinger, who in 1933 shared the Nobel Prize with Paul Dirac, introduced the conventional idea. Albert Einstein proposed a situation that came to known as the EPR (Einstein-Podolsky-Rosen) paradox, where he called attention to the fact that while it was impossible to know whether a single photon would pass or be absorbed by a filter paired photon. Would a subject to the same polarization test always being entangled. The experiment simply succeeded, where the entangle went of a single/two photons was observed and this has been used in some applications in quantum cloning, quantum teleportation, measurement and cryptography.

Quantum information was theoretically well established by Bennett et al. [1]. The proposed scheme was also presented for quantum cryptography by the same authors [2, 3]. This area of research has now been now investigated theoretically [4] or experimentally. It is expected that the implemented systems will have a wide range of applications in the near future. The applications of the phenomena include quantum cryptography, quantum teleportation [5], quantum key and quantum CODEC (code and decode). Zellinger et al. [6] have demonstrated that photon can be transported using a classical channel by a Mach-Zhender Interferometer (MZI), where photons in linear or circular polarization states can form the entangled pairs. Quantum cryptography through free space, wireless or optical fiber has been reported. Weinfurter et al. [7] have shown that quantum cryptography can be realized by using a single photon transmission in a light wave channel. Recently he has demonstrated that the four states of polarized light can be form quantum cryptography using such a simple arrangement. Suchat and Yupapin [8] have also shown that by using a classical MZI with one arm modulated by a $LiNbO_3$ crystal a single photon can be generated. Brendel et al. [9] have generated pulse polarization entanglement or pulse energy time entanglement by MZI in a delay circuit. Takesue et al. [10] have also shown the same results

using Michelson interferometer. Silberhorn et al. [11] have reported on the generation of a continuous variable entanglement using an optical fiber interferometer, where the Kerr nonlinearity in the fiber is exploited for the generation of two independent squeezed beams. Since the nonlinearity of optical ring resonators has shown great promise for a variety of applications such as optical time delay [12] and optical switching [13].

This research is present the quantum entangle photons via the transmission by using a classical channel via Mach-Zehnder Interferometer (MZI), in which data between two orthogonal states. The two states are horizontal (H) and vertical (V) polarization a photon. In this, using the time bin entanglement is in optics. We have made a similar system to that described in reference [11] but we use a nonlinear fiber optic ring resonator for the delay and interference signals. Which when polarized generates the pulsed polarization-entangled photons. This is a new scheme that uses an all fiber optic system without any optical pumping part from polarized light pulses. We have demonstrated that an all fiber optic MZI incorporating a nonlinear fiber optic ring resonator can be used to generate pulsed polarization-entangled photon pairs. Which are based on the conventional time-bin entanglement arrangement [9].

1.2 Objective of the Study

This research is conducted in order to

1.2.1 Study process of Mach Zehnder interferometer.

1.2.2 Study the quantum entangle photons

1.2.3 Study the time bin entanglement.

1.3 Scope of Study

The aim of this study is to show that the entangled photons study based on Mach Zehnder interferometer, and then we will show properties of the experiment methods. We will then make a conclusion the properties of each method.

Formulating a written thesis was based on the information presented here and involved the following procedures. In chapter 2, we provided the theoretical background, which involved definitions and theorems, which were later used in chapter 3. Chapter 3 focused on presenting information which showed that the time bin entangle photon is a well posed theoretical and method of the experiment. In chapter 4 we presented experiment of Mach Zehnder interferometer;

entangle photons and time bin entanglement photon respectively. In chapter 5 we presented results and discussion for this the experiment set up in Mach Zehnder interferometer and entangles photons. Finally, we made a conclusion and suggestion in chapter 6.

1.4 Process of the Study

1.4.1 Study the theory of Mach Zehnder interferometer.

1.4.2 Study the theory of quantum entangles photons.

1.4.3 Study the theory of the time bin entanglements.

1.4.4 Set up on the Mach Zehnder interferometer, quantum entangles photons, the time bin entanglement.

1.4.5 Conclude and discuss the results

1.5 Expected Results

1.5.1 Important physical meaning; i.e state of quantum and entangle photon will be clearly understood.

1.5.2 Effects of temperature, intensity, modulation frequency, and external applied will be acknowledged.

1.5.3 Potential advantages of Mach Zehnder interferometer and entangle photon are utilized.

CHAPTER 2

THEORETICAL BACKGROUND

The main objective of this study is to understand the interferometer, photons, fiber optic Mach-Zehnder interferometer and fiber optics ring resonator, in this chapter, the important theories are presented.

2.1 Interferometer

2.1.1 Beamsplitter

We assume that the input beam is a traveling coherent state $|Ain\rangle$. A beamsplitter will maintain the mode properties. The frequencies of the light, the size of the beam, the curvature of the wavefront are all preserved. The direction of propagation is given by geometrical considerations. The polarizing properties of the mirror can be neglected by assuming that that the incoming light is either P or S polarized. The calculation for a different polarization is treated as a linear combination of these special cases. Thus a beamsplitter can be simply described by a transformation from two input modes $|Ain\rangle$ and $|Au\rangle$ into two output mode $|At\rangle$ and $|Ar\rangle$. The properties to consider are the numbers for the photon flux N_{Ain}, N_{Au}, N_{At} and N_{Ar} and the variances of these modes. Using the convention for the properties of a beam splitter, we describe the proper of the beamsplitter by the intensity reflection coefficient ε [15]

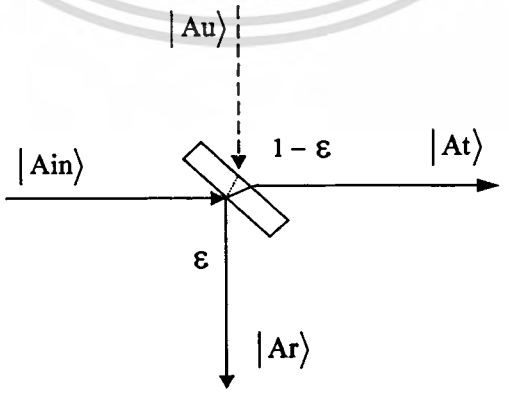

Figure 2.1 The beamsplitter in the quantum operator model.

When the beam splitter matrix is,

$$M=\begin{pmatrix}\sqrt{\varepsilon} & \sqrt{1-\varepsilon}\\ \sqrt{1-\varepsilon} & -\sqrt{\varepsilon}\end{pmatrix} \tag{2.1}$$

We can use a matrix definition for the definition of a beamsplitter,

$$\begin{pmatrix}|A_r\rangle\\ |A_t\rangle\end{pmatrix}=M\begin{pmatrix}|A_{in}\rangle\\ |A_u\rangle\end{pmatrix}=\begin{pmatrix}M_{ri} & M_{tu}\\ M_{ti} & M_{ru}\end{pmatrix}\begin{pmatrix}|A_{in}\rangle\\ |A_u\rangle\end{pmatrix} \tag{2.2}$$

The reflected and transmitted modes are set respectively as

$$\begin{aligned}\hat{A}_r&=\sqrt{\varepsilon}\hat{A}_{in}+\sqrt{1-\varepsilon}\hat{A}_u\\ \hat{A}_t&=\sqrt{1-\varepsilon}\hat{A}_{in}-\sqrt{\varepsilon}\hat{A}_u\end{aligned} \tag{2.3}$$

The variance of the photon flux of the reflected mode can be calculated directly as:

$$\begin{aligned}VN_{Ar}&=\left\langle\hat{A}_r^{\dagger}\hat{A}_r\hat{A}_r^{\dagger}\hat{A}_r\right\rangle-\left\langle\hat{A}_r^{\dagger}\hat{A}_r\right\rangle^2\\ &=\left\langle\left(\sqrt{\varepsilon}\hat{A}_{in}^{\dagger}+\sqrt{1-\varepsilon}\hat{A}_u^{\dagger}\right)\left(\sqrt{\varepsilon}\hat{A}_{in}+\sqrt{1-\varepsilon}\hat{A}_u\right)\right.\\ &\quad\left.\left(\sqrt{\varepsilon}\hat{A}_{in}^{\dagger}+\sqrt{1-\varepsilon}\hat{A}_u^{\dagger}\right)\left(\sqrt{\varepsilon}\hat{A}_{in}+\sqrt{1-\varepsilon}\hat{A}_u\right)\right\rangle\end{aligned}$$

$$\begin{aligned}VN_{At}&=\left\langle\hat{A}_t^{\dagger}\hat{A}_t\hat{A}_t^{\dagger}\hat{A}_t\right\rangle-\left\langle\hat{A}_t^{\dagger}\hat{A}_t\right\rangle^2\\ &=\left\langle\left(\sqrt{1-\varepsilon}\hat{A}_{in}^{\dagger}-\sqrt{\varepsilon}\hat{A}_u^{\dagger}\right)\left(\sqrt{1-\varepsilon}\hat{A}_{in}-\sqrt{\varepsilon}\hat{A}_u\right)\right.\\ &\quad\left.\left(\sqrt{1-\varepsilon}\hat{A}_{in}^{\dagger}-\sqrt{\varepsilon}\hat{A}_u^{\dagger}\right)\left(\sqrt{1-\varepsilon}\hat{A}_{in}-\sqrt{\varepsilon}\hat{A}_u\right)\right\rangle\end{aligned} \tag{2.4}$$

for the case of a simple beamsplitter we can set $|A_u\rangle=|0\rangle$. A total of 16 terms appear in the expansion, each term contains a sequence of four operators. This expression can be simplified. In particular all terms which contain 3 operators of one mode and 1 operator of the other mode have the expectation value 0. Other terms have to be expanded using the commutator rules, and the equation simplifies to

$$V1_{Ar} = \varepsilon V1_{Au} + (1-\varepsilon)V1_{Ain}$$
$$V1_{At} = (1-\varepsilon)V1_{Au} + \varepsilon V1_{Ain} \qquad (2.5)$$

For a simple beamsplitter the result obviously does not depend on the quadrature of the vacuum. It should be noted that equation (2.5) also holds if a squeezed vacuum state enter through the unused, second port. In this case the quadrature which is detected is of importance. It will depend exactly on the type of mirror that is used, that means the actual phase shift between the transmitted and the reflected light.

2.1.2 Mach Zehnder interferometer

Generally, the operating medium can be considered the quantum can be use to described the optical behaviors. The quantum property of devices is very impressive because the device dimension can be reducing into atomic size with very large capacity of information.

The input signal can be modulated with baseband signals and carrier then multiplex before entering to the instrument. All information can be transformed into a light beam and transmit to the destination. The selection of the required information is formed by the optical signal processing technique.

An interferometer is an instrument that has been widely used either in classical or modern optics. The quantum model of the Mach Zehnder interferometer is as shows in Figure 2.2

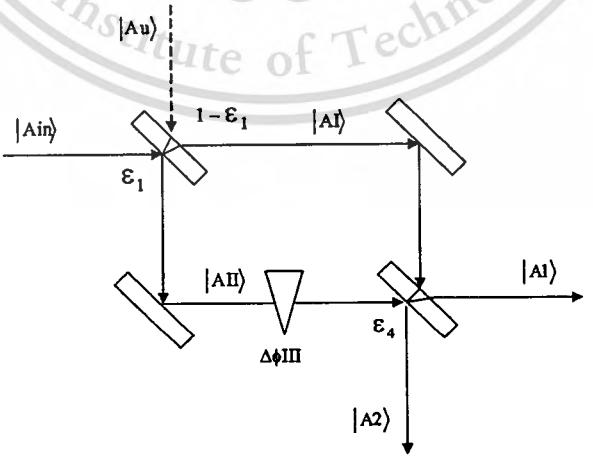

Figure 2.2 Description of an interferometer in the generalized model

The interferometer is illuminated by a mode $|\mathrm{Ain}\rangle$, inside we have the modes $|\mathrm{AI}\rangle$ and $|\mathrm{AII}\rangle$. After recombination we have the two output modes $|\mathrm{A1}\rangle$ and $|\mathrm{A2}\rangle$ which are detected individually. As with the classical model the case of a Mach Zehnder interferometer with a phase difference $\Delta\phi$ is treated first. The results can be generalized to any other interferometer and to application where $\Delta\phi$ is a function of time or space. The internal states are linked to the input states via

$$\begin{aligned}|\mathrm{AI}\rangle &= \sqrt{1-\varepsilon_1}\,|\mathrm{Ain}\rangle - \sqrt{\varepsilon_1}\,|\mathrm{Au}\rangle \\ |\mathrm{AII}\rangle &= \sqrt{\varepsilon_1}\,|\mathrm{Ain}\rangle + \sqrt{1-\varepsilon_1}\,|\mathrm{Au}\rangle\end{aligned} \tag{2.6}$$

The out put state are liked to the internal states via

$$\begin{aligned}|\mathrm{A1}\rangle &= \exp(i\Delta\phi)\sqrt{1-\varepsilon_4}\,|\mathrm{AII}\rangle - \sqrt{\varepsilon_4}\,|\mathrm{AI}\rangle \\ |\mathrm{A2}\rangle &= \exp(i\Delta\phi)\sqrt{\varepsilon_4}\,|\mathrm{AII}\rangle + \sqrt{1-\varepsilon_1}\,|\mathrm{AI}\rangle\end{aligned} \tag{2.7}$$

For the balanced interferometer we can set $\varepsilon_1 = \varepsilon_4 = \frac{1}{2}$ and the equation can be combined to

$$\begin{aligned}|\mathrm{A1}\rangle &= \exp(i\Delta\phi/2)\left(\cos(\Delta\phi/2)\,|\mathrm{Ain}\rangle - i\sin(\Delta\phi/2)\,|\mathrm{Au}\rangle\right) \\ |\mathrm{A2}\rangle &= \exp(i\Delta\phi/2)\left(i\sin(\Delta\phi/2)\,|\mathrm{Ain}\rangle + \cos(\Delta\phi/2)\,|\mathrm{Au}\rangle\right)\end{aligned} \tag{2.8}$$

In order to determine the photon flux, for example at output $\hat{A}_2$, we have to evaluate the operator

$$\begin{aligned}\hat{N}_{A2} = \hat{A}_2^{\dagger}\hat{A}_2 &= \sin^2(\Delta\phi/2)\hat{A}_{in}^{\dagger}\hat{A}_{in} + \cos^2(\Delta\phi/2)\hat{A}_u^{\dagger}\hat{A}_u \\ &\quad - i\sin(\Delta\phi/2)\cos(\Delta\phi/2)\left(\hat{A}_{in}^{\dagger}\hat{A}_u - \hat{A}_u^{\dagger}\hat{A}_{in}\right)\end{aligned} \tag{2.9}$$

The last term in this equation describes the interference one would expect in the presence of a second laser beam illuminating the input port $|\mathrm{Au}\rangle$. When expect input state is the vacuum state the expectation value for this term is, of course, zero. In addition, the value of $\langle \hat{A}_u^{\dagger}\hat{A}_u \rangle$ is zero since the vacuum input has no photon flux. Thus the average intensities at the two outputs are simply

$$N_{A1} = N_{Ain}\cos^2(\Delta\phi/2)$$
$$N_{A2} = N_{Ain}\sin^2(\Delta\phi/2) \quad (2.10)$$

The interferometer distributes the energy between the two output ports. The ratio of the distribution can be adjusted by the differential phase $\Delta\phi$. The calculation of the fluctuations requires the evaluation of

$$VN_{A2} = \left\langle \hat{A}_2^{\dagger}\hat{A}_2\hat{A}_2^{\dagger}\hat{A}_2 \right\rangle - \left\langle \hat{A}_2^{\dagger}\hat{A}_2 \right\rangle^2 \quad (2.11)$$

in these calculations we have to evaluate expectation values for the square of the last term of equation (2.9), which is non zero, even for a vacuum state. Under the assumptions that: (i) the second port is not used, $|Au\rangle = 0$, (ii) the photon flux of input beam is dominant $(N_{Ain} >> 1)$ and (iii) the laser beam is coherent, we obtain

$$VN_{A1} = \cos^2(\Delta\phi/2)N_{Ain}\left\langle \Delta X2_u^2 \right\rangle$$
$$VN_{A2} = \sin^2(\Delta\phi/2)N_{Ain}\left\langle \Delta X2_u^2 \right\rangle \quad (2.12)$$

The fluctuation of the two outputs is proportional to the average photon fluxes. The sizes of the fluctuations reflect the division of the flux between the two outputs. The output can be interpreted as a beat between the coherent input beam and the vacuum state with $\left\langle \Delta X2_u^2 \right\rangle = 1$. For an interferometers with one input beam we obtain

$$Vl_{A1} = \cos^2(\Delta\phi/2)$$
$$Vl_{A2} = \sin^2(\Delta\phi/2) \quad (2.13)$$

2.1.3 Noise properties of interferometers

For small change $\delta\phi$ of phase shift $(\delta\phi << \pi)$ the change in the optical flux at the detector is equal to the first derivative of the output photon flux in regard to the phase multiplied with $\delta\phi$ [15]

$$\delta\phi = \delta\phi\frac{d(N_{A2})}{d\phi}$$
$$= \delta\phi 2\cos(\Delta\phi/2)\sin(\Delta\phi/2)\frac{1}{2}N_{Ain} \approx \frac{\Delta\phi}{2}\sin(\Delta\phi)N_{Ain} \quad (2.14)$$

An AC detector measures the signal power p_{sig}, which is proportional to the square of the change in optical power and includes τ, the inverse of the detection bandwidth.

$$p_{sig} = \left(\frac{\delta\phi}{2}\sin(\Delta\phi)N_{Ain\tau}\right)^2 \tag{2.15}$$

Where $\delta\phi$ is the small phase shift $(\delta\phi << \pi)$ the signal can be compared with the variance of the photon number, or the quantum noise on the detector

$$p_{qnoise} = VN_{A2} = \sin^2(\Delta\phi/2)N_{Ain\tau} \tag{2.16}$$

And we can evaluate the signal to noise ratio

$$SNR = \frac{\sin^2(\Delta\phi)}{\sin^2(\Delta\phi/2)}N_{Ain\tau}\frac{\delta\phi^2}{4} \tag{2.17}$$

Which has the largest value when $\Delta\phi = 0, 2\pi$ where the output optical power is at a minimum.

The phase change $\Delta\phi$ is introduced in the interferometer system relating to the optical path difference between two paths of traveling light along the modulated medium. The output signals characteristics are studied in order to use to model for optical signal processing devices such as filter, switching, multiplexer / demultiplexer etc.

The term of phase change $\Delta\phi$ can be induce by force, vibration, temperature or electro-optic application on one path of traveling light which can be replaced by variety of optical fiber or optical materials, thus

$$\Delta\phi = \frac{2\pi}{\lambda}nl \tag{2.18}$$

When λ is wavelength of light source, n is refractive index and l is a length of the medium

$$\delta\phi_{QNL} = \frac{1}{\sqrt{N_{Ain}\sin^2(\Delta\phi/2)}} \tag{2.19}$$

When $\Delta\phi = \pi$ (dark fringe operation)

$$\delta\phi_{QNL} = \frac{1}{\sqrt{N_{Ain}}} \tag{2.20}$$

2.1.4 $LiNbO_3$ modulated

The term phase change can be changed i.e. modulated by using a $LiNbO_3$ crystal with a drive voltage from ac (alternative current) signal source. The relationship between the output frequency and applied voltage is written in the form as [18]

$$V_\pi(f) = V_\pi(dc)10^{-OR(f)/20} \tag{2.21}$$

Where OR is the optical response (in dB), f is input drive frequency and V_π is voltage required for π phase shift.

The detected ac signal is largest when the change in power is most rapidly changed, that is when $\Delta\phi = \frac{\pi}{2}$, at the center point between the maximum and minimum peak of the interference fringe. The signal can be compared with the variance of the photon number, or the quantum noise on the detector.

2.2 Fiber Optic Mach-Zehnder Interferometer

The Mach-Zehnder configuration is an intrinsic sensor based on the interference between a sensing and a reference wave. The two-beam interferometer uses a laser diode as the source of coherent light, which is coupled into a single mode fiber. The light is then split equally into two fibers by a 3-dB coupler. One arm of the Mach-Zehnder interferometer is the sensing arm while the other is the reference. The reference fiber is kept protected from the desired perturbation to be measured and light passes through this arm normally. The sensing fiber is used to monitor the perturbation. Two complementary outputs are available for signal processing. The electric fields of the two light waves can be expressed as

$$E_r = E_0 e^{i\omega_0 t} \text{ and } E_s = E_0 e^{i(\omega_0 t + \Delta\phi)} \tag{2.22}$$

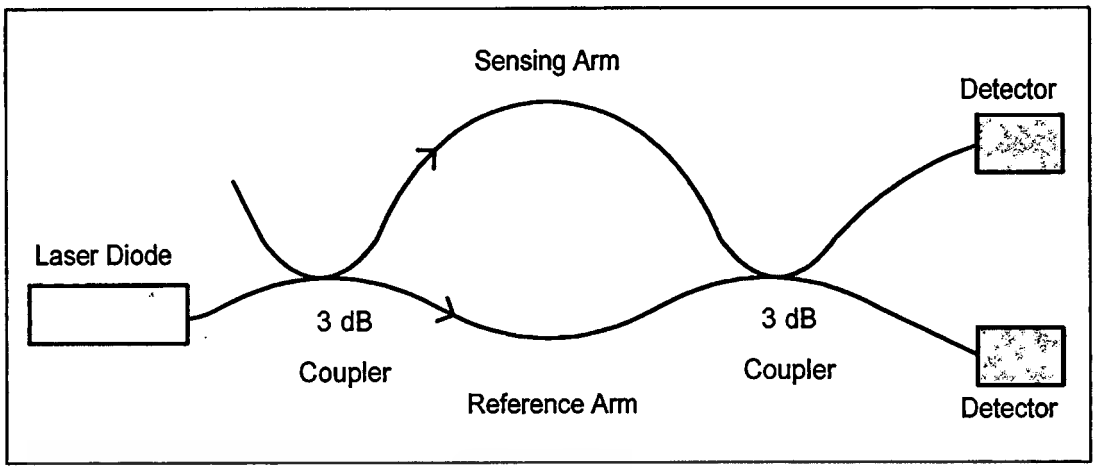

Figure 2.3 Fiber Optic Mach-Zehnder Interferometer

Where E_r is the reference wave, E_s is the sensing wave, and $\Delta\phi$ is the phase difference induced by the sensing fiber. At the photo detector, the intensity is given by

$$I = \langle E_r^2 \rangle + \langle E_s^2 \rangle + 2\langle E_r E_s \rangle \tag{2.23}$$

Where $\langle\ \rangle$ represents the time integration performed by the photo detector. This equation reduces to

$$I = I_0(1 + \cos\Delta\phi) \tag{2.24}$$

Where $I_0 \alpha\ E_0^2$ and we have assumed in the ideal conditions of equal splitting ratios, no coherence or polarization effects, and no losses.

The information is contained in the phase difference between the two waves. The phase corresponding to a length of fiber L is

$$\phi = kn_{eff}L \tag{2.25}$$

Where $k = 2\pi/\lambda$ is the propogtion constant in air, λ is the laser diode-emitting wavelength, and n_{eff} is the fiber's effective refractive index. if the desired measured is X, then the change in ϕ may be represented by

$$\Delta\phi = kL\frac{dn_{eff}}{dX}\Delta X + kn_{eff}\frac{dL}{dX}\Delta X \tag{2.26}$$

If the coefficients $\frac{dn_{eff}}{dX}$ and $\frac{dL}{dX}$ for the sensing fiber are known, ΔXcan be found from the output signal, expressed by Equation (2.24).

In this configuration, quantities such as strain, force, pressure, and temperature can be measured directly. Other quantities such as magnetic field, acoustic pressure, electric field, and current can be measured indirectly by attaching the sensing fiber to materials that respond to these parameters. The output of the sensor, Equation (2.24), is sinusoidal and is shown in Figure 2.4. The signal goes through one period for every 2π shift in $\Delta\phi$. This period is referred to as one fringe.

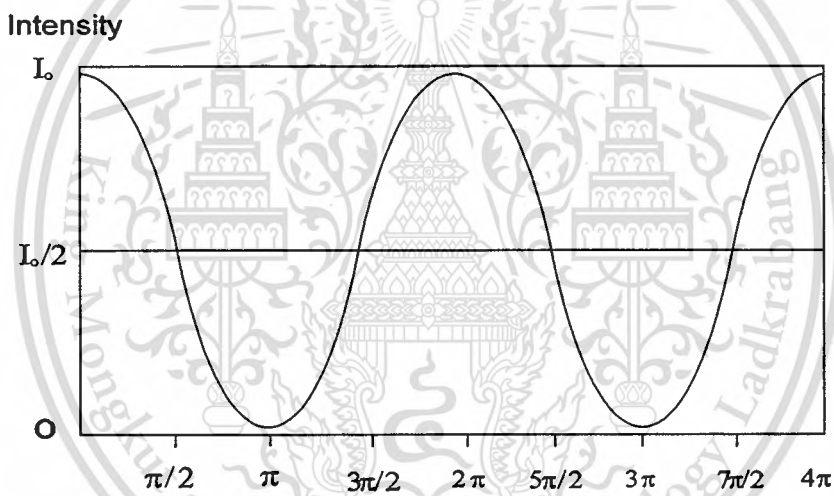

Figure 2.4 Mach-Zehnder Interferometer Output

In this configuration, quantities such as strain, force, pressure, and temperature can be measured directly. Other quantities such as magnetic field, acoustic pressure, electric field, and current can be measured indirectly by attaching the sensing fiber to materials that respond to these parameters.

2.3 Fiber Optics Ring Resonator

We analyze the device illustrated in Fig. 2.5. We describe the coupling of light into and out of the resonator in terms of generalized beam splitter relations of the form

$$E_2 = rE_1 + itE_3 \tag{2.27}$$

$$E_4 = rE_3 + itE_1 \tag{2.28}$$

where r and t are taken to be real quantities that satisfy the relation $r^2 + t^2 = 1$ and the fields are defined with respect to the reference points indicated in Figure 2.5. [12]

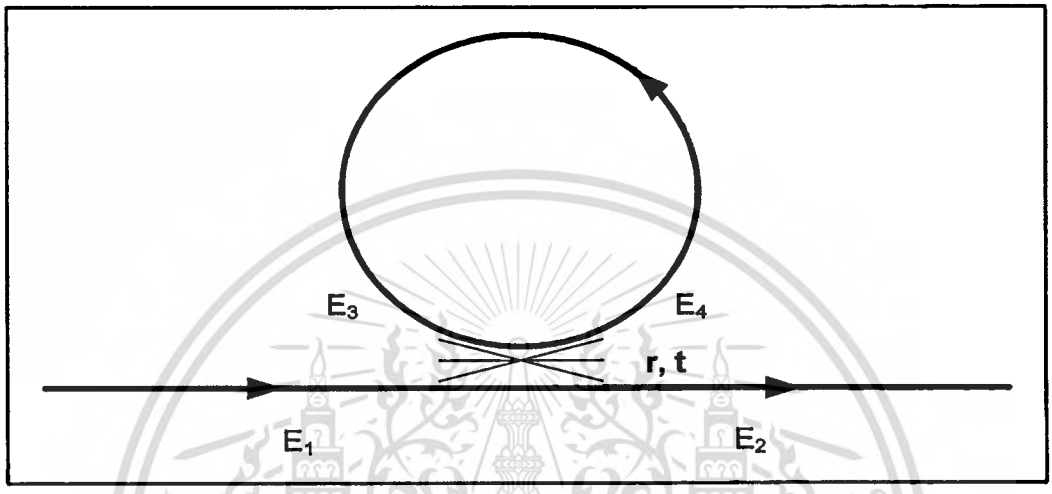

Figure 2.5 Geometry of a fiber ring resonator.

In addition, we describe the circulation of light within the resonator in terms of the round-trip phase shift ϕ and the amplitude transmission factor τ such that

$$E_2 = \tau \exp(i\phi) E_4 \tag{2.29}$$

The round-trip phase shift ϕ can be interpreted as $\phi = kL$, where $k = 2\pi n/\lambda$, n is the effective refractive index of the fiber mode, λ is the vacuum wavelength of the incident light, and L is the circumference of the fiber ring. Equations (2.27)–(2.29) can be solved simultaneously to find that the input and output fields are related by the complex amplitude transmission

$$\frac{E_2}{E_1} = \exp[i(\pi + \phi)] \frac{\tau - r\exp(-i\phi)}{1 - r\tau\exp(i\phi)} \tag{2.30}$$

The intensity transmission factor is given by the squared modulus of this quantity

$$T = \left|\frac{E_2}{E_1}\right|^2 = \frac{\tau^2 - 2r\tau\cos\phi + r^2}{1 - 2r\tau\cos\phi + r^2\tau^2} \tag{2.31}$$

Note that the on-resonance transmission $(\phi = 0)$ drops to zero for the situation $r = \tau$. In this case, the internal losses are equal to the coupling losses, and the resonator is said to be critically coupled. For $r > \tau$, the resonator is said to be undercoupled and for $r < \tau$ the resonator is said to be overcoupled. The phase of the transmitted light is given by the argument of (2.30) as follows:

$$\begin{aligned}\Phi &= \arg\left(\frac{E_2}{E_1}\right) \\ &= \pi + \phi + a\tan\left(\frac{r\sin\phi}{\tau - r\cos\phi}\right) + a\tan\left(\frac{r\tau\sin\phi}{1 - r\tau\cos\phi}\right)\end{aligned} \tag{2.32}$$

Near each resonance, the phase undergoes a rapid variation with respect to the round-trip phase shift. This round-trip phase shift may be interpreted as a frequency detuning normalized through multiplication by the round-trip time.

2.4 Photons

The basic postulate of the quantum interpretalation is that electromagnetic radiation consists of particle-like discrete bundles of energy called photons or quanta. Each photon has an energy E that depends only on the frequency ν of the radiation and is given by

$$E = h\nu = h\frac{c}{\lambda} \tag{2.33}$$

where $h = 6.626\times10^{-34}$ J.s is Planck's constant. Each photon interact an all-or-nothing manner; it either gives up all its energy or none of it.

Since photons travel at the speed of light, they must, according to relativity theory, have zero rest mass: hence, their energy is entirely kinetic. If a photon exists, then it moves at the speed of light, c; if it ceases to move with speed c, it ceases to exist. For $m_0 = 0$, the relativistic momentum-energy relation becomes $E = pc$. Thus, each photon has a momentum of

$$p = \frac{E}{c} = \frac{h\nu}{c} = \frac{h}{\lambda} \tag{2.34}$$

From the quantum point of view, a beam of electromagnetic energy is composed of photons traveling at the speed c. the intensity of the beam will be proportional to the number of photons crossing a unit area per unit time. Hence, if the beam is monochromatic (one frequency), the intensity I will be given by

$$I = (\text{energy of one photon}) \times \frac{\text{number of photons}}{\text{area} \times \text{time}} \tag{2.35}$$

Finally, we note for convenience in calculations the following expression in nonstandard units:

$$h = 4.136 \times 10^{-15} \text{eV.s} \tag{2.36}$$

$$hc = 12.4 \text{keV.A}^0 \tag{2.37}$$

where $1\text{ev} = 10^{-3}\text{keV} = 1.602 \times 10^{-19}\text{J}$ and $1\text{A}^0 = 10^{-10}\text{m}$.

CHAPTER 3

TIME BIN ENTANGLEMENT

The main objective of this study is to understand the entangled photons and time bin entanglement, in this chapter, the important theories are presented.

3.1 Entangled Photons

An excited atom emits two photons that come out back to back from the Einstein Podolsky Rosen (EPR) source [11], with vanishing angular momentum and even parity. If $|x\rangle$ and $|y\rangle$ are horizontal and vertical linear polarization states of the photon, then have seen that

$$|+\rangle = \frac{1}{\sqrt{2}}\left(|x\rangle + i|y\rangle\right)$$
$$|-\rangle = \frac{1}{\sqrt{2}}\left(i|x\rangle + |y\rangle\right) \tag{3.1}$$

are the eigenstates of helicity. For two photons, one propagating light is in the $+\hat{z}$ direction and other in the $-\hat{z}$ direction. The states

$$|+\rangle_A|-\rangle_B$$
$$|-\rangle_A|+\rangle_B \tag{3.2}$$

are invariant under rotations about $\hat{z}$. (The photons have opposite values of J_z, but the same helicity, since they are propagating in opposite directions.) Under a reflection in the y–z plane, the polarization states are modified according to

$$|x\rangle \to -|x\rangle \ , |+\rangle \to +i|-\rangle$$
$$|y\rangle \to |y\rangle \ , \ |-\rangle \to -i|+\rangle \tag{3.3}$$

Therefore, the parity eigenstates are entangled states

$$\frac{1}{\sqrt{2}}\left(|+\rangle_A|-\rangle_B \pm|-\rangle_A|+\rangle_B\right) \tag{3.4}$$

The state with $J_z = 0$ and even parity, then, expressed in terms of the linear polarization states, is

$$-\frac{i}{\sqrt{2}}\left(|+\rangle_A|-\rangle_B \pm|-\rangle_A|+\rangle_B\right) = \frac{1}{\sqrt{2}}\left(|xx\rangle_{AB} + |yy\rangle_{BA}\right)_n = |\phi^+\rangle_{AB} \tag{3.5}$$

Because of invariance under rotations about $\hat{z}$, the state has this form irrespective of how we orient the x and y axes. We can use a polarization of either photon along any axis in the xy plane. Let $|x(\theta)\rangle$, and $|y(\theta)\rangle$ denote the linear polarization eigenstates along axes rotated by angle θ relative to the canonical x and y-axes. We may define an operator as (the analog of $\vec{\sigma}\cdot\hat{n}$)

$$\tau(\theta) = |x(\theta)\rangle\langle x(\theta)| - |y(\theta)\rangle\langle y(\theta)| \tag{3.6}$$

Which has these polarization states as eigenstate with respective eigenvalues as

$$|x(\theta)\rangle = \begin{pmatrix}\cos\theta\\ \sin\theta\end{pmatrix},$$

$$|y(\theta)\rangle = \begin{pmatrix}-\sin\theta\\ \cos\theta\end{pmatrix} \tag{3.7}$$

Let $|H\rangle$ and $|V\rangle$ be two polarization states of photon, which are sent from Alice to Bob along two separated channels. We shall take two orthogonal states $|\psi_+\rangle$ and $|\psi_-\rangle$, linear combinations of $|H\rangle$ and $|V\rangle$, to represent bit value "0" and bit value "1," respectively:

$$|\psi_+\rangle = \frac{1}{\sqrt{2}}(|H\rangle + |V\rangle) \tag{3.8}$$

$$|\psi_-\rangle = \frac{1}{\sqrt{2}}(|H\rangle - |V\rangle) \tag{3.9}$$

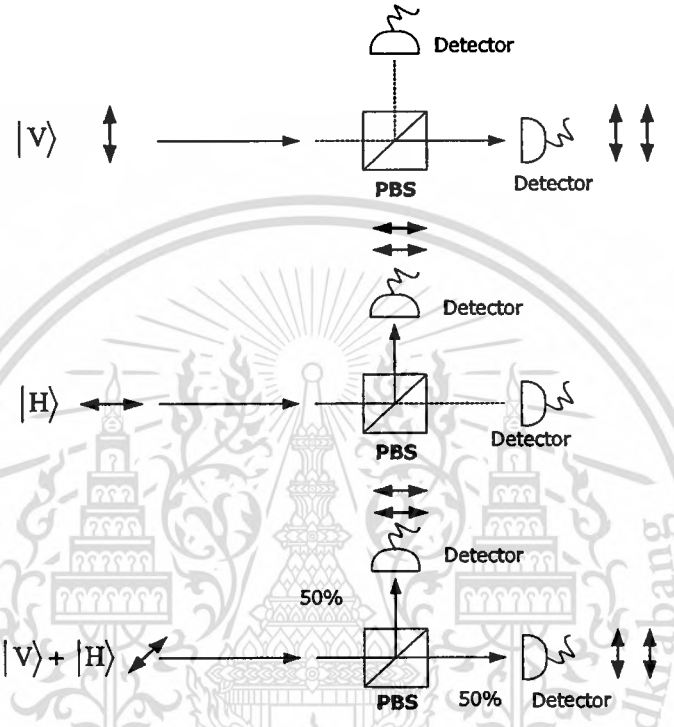

Figure 3.1 Schematic diagram of a single photon entangled state.

Alice sends to Bob either $|\psi_+\rangle$ or $|\psi_-\rangle$. The two localized states, $|H\rangle$ and $|V\rangle$, are not sent together, but $|V\rangle$ is delayed for some time τ. For simplicity, we choose τ to be larger than the traveling time of the particles from Alice to Bob, θ. Thus $|V\rangle$ starts traveling towards Bob only when $|H\rangle$ already has reached Bob, such that the two wave packets and never found together in the transmission channels.

We shall consider a particular implementation of our scheme. The setup (Figure 3.2) consists of a Mach-Zehnder interferometer, with ϕ_A and ϕ_B as phase delays which and equal to time delay. Alice can transmit an information bit by sending either from a single particle or from short pulse of laser source, where the sending time t is random and registered by Alice for later use. The particle passes through the first beam splitter BS1 and evolves into a superposition of

two localized wave packets. Finally, the two wave packets arrive simultaneously to the second beam splitter BS2 and interfere. A particle started in state $|\psi_+\rangle$ emerges at the detector D1, and a particle started in state $|\psi_-\rangle$ emerges at the detector D2. Bob. The detection of the arriving particle receives the bit sent by Alice: D1 was activated by mean of 0 and D2 mean 1, i.e. he registers the receiving time of the particle.

From Figure 3.2, consider a Mach-Zehnder interferometer when one mode of the input polarization states is traveling into the modulator i.e. external pumping power. The coupling mode occurs due to the change of the input orientation angle ($\Delta\phi$), which is caused by the change of the optical output power. When the interferometer is at a dark fringe position, this is different from the one used in a classical interferometer with intensity independent noise. The reason is that the signals and noises disappear at $\Delta\phi = 0$, while the quantum noise more rapidly disappears.

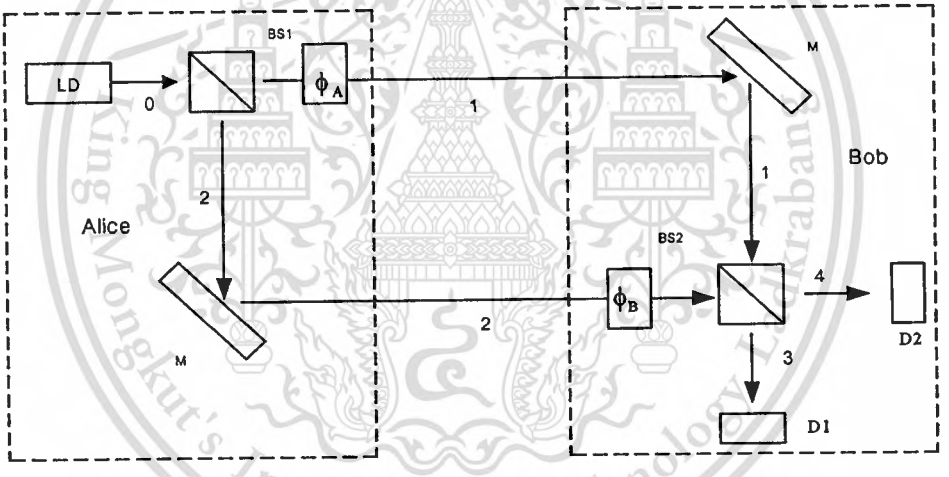

Figure 3.2 Encryption scheme bases on a Mach-Zehnder interferometer. LD: Laser diode, BS: Beam splitter, Ms: Mirrors, Ds: Detectors.

Given $I_1 = I_2$ is the output intensity of light in Mach-Zehnder interferometer, and $I_0 = I_1 + I_2 = I_3 + I_4$. Consider a perfect monochromatic light source from laser diode; the signal amplitude is expressed as in equation (3.10).

$$E_0 = \sqrt{2I_0}\cos(\omega t) \tag{3.10}$$

According to Figure 3.2, E_i, i =1,2,3, 4 are the signal amplitudes of the transmitted light beams at the given positions in MZI, where l is coherence length and ω is an angular frequency. Consider that the first beam splitter (BS1), yields

$$E_0 = \sqrt{2I_0}\cos\left(\omega\left[t-\frac{l_0}{c}\right]\right) \tag{3.11}$$

$$E_1 = \sqrt{I_0}\cos\left(\omega\left[t-\frac{l_0}{c}\right]\right) \tag{3.12}$$

$$E_2 = \sqrt{I_0}\cos\left(\omega\left[t-\frac{l_0}{c}\right]\right) \tag{3.13}$$

and the second beam splitter (BS2)

$$E_1 = \sqrt{I_0}\cos\left(\omega\left[t-\frac{l_0}{c}-\frac{l_1}{c}\right]\right) \tag{3.14}$$

$$E_2 = \sqrt{I_0}\cos\left(\omega\left[t-\frac{l_0}{c}-\frac{l_2}{c}\right]\right) \tag{3.15}$$

We now consider E_3

$$E_3 = \sqrt{\frac{I_0}{2}}\left\{\cos\left(\omega\left(t-\frac{l_0+l_1}{c}\right)\right)+\cos\left(\omega\left(t-\frac{l_0+l_2}{c}\right)\right)\right\} \tag{3.16}$$

$$E_3 = \sqrt{2I_0}\cos\left(\omega\left(t-\frac{2l_0+l_1+l_2}{2c}\right)\right).\cos\left(\omega\frac{l_1-l_2}{2c}\right) \tag{3.17}$$

$$I_3 = \left\langle E_3^2\right\rangle_t = I_0\cos^2\left(\omega\frac{l_1-l_2}{2c}\right) = I_0\cos^2\left(\frac{\phi_A-\phi_B}{2}\right) \tag{3.18}$$

$$I_4 = I_0\sin^2\left(\frac{\phi_A-\phi_B}{2}\right) \tag{3.19}$$

The normalized output is formed by substituting ϕ_A and ϕ_B into Equation (3.18), (3.19), and yields.

ϕ_A	0	$\frac{\pi}{2}$	π	$\frac{3\pi}{2}$	2π
ϕ_B	0	0	0	0	0
$\frac{I_3}{I_0}$	1	$\frac{1}{2}$	0	$\frac{1}{2}$	1
$\frac{I_4}{I_0}$	0	$\frac{1}{2}$	1	$\frac{1}{2}$	0

This shows that Eve, who has access to the channels but not to the sites of Alice and Bob, cannot extract any information without introducing detectable distortions in the transmission. The data are encoded in the relative phase between the two polarization states $|H\rangle$ and $|V\rangle$. Therefore, the phase must be the same as time, which means the two-wave packet must arrive together at BS2 at the correct time.

3.2 Time-Bin Entangled Photons

A conventional fiber optic Mach-Zehnder interferometer is configured as an intrinsic sensor based on the interference between a sensing and a reference signal. A standard two-beam interferometer uses a laser diode as a coherent light source.

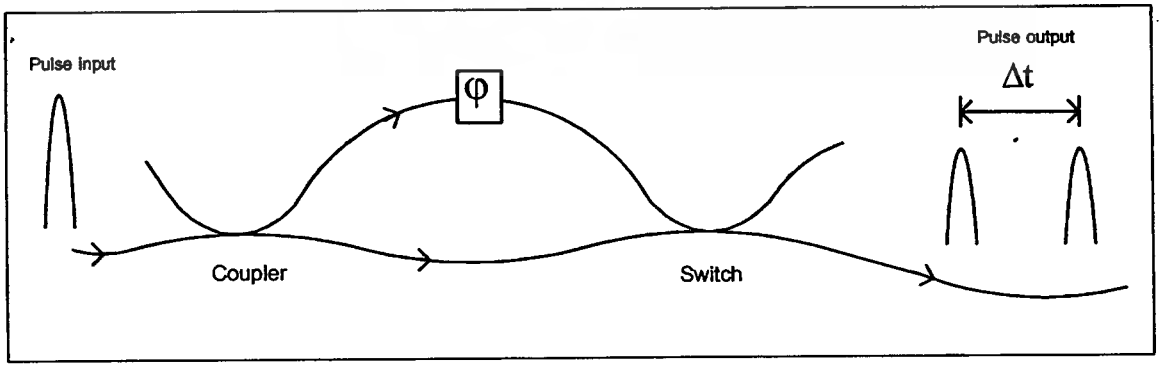

Figure 3.3 A schematic of fiber optic Mach-Zhender interferometer.

To understand a system of all fiber optic interferometer, it is useful to start with the simple device, which can be entirely understood in terms of classical linear optics in Figure 3.3. Let a 1-photon pulse enter into the device from left-hand side via one end of the coupler, which is assumed that it duration time is shot compared to the length difference of the interferometer arms. The incoming pulses were split by the first fiber-coupler between a short and a longer fiber path, in order to form a temporally separated pulse pair. The path lengths were chosen such that a relative time delay of 9.9 μs was obtained between the pair of pulses coupled into the transmission fiber via the second coupler. A phase shifter consisting of which could be varied by polarization control fiber (PC). The output pulses consists of two well-separated pulses which denote them shot and long respectively, which is presented the basis of quantum bit (qubit) space, similarly to the usual vertical $|V\rangle$ and horizontal $|H\rangle$ linear polarization states. The relative norm and phase of the coefficients α and β are determined by the coupling ratio (η) of the coupler (beam splitter) and the phase φ of the phase shifter, respectively. Hence, any state of the two-dimensional Hilbert space spanned by the basic state can be prepared and analyzed. The duration time difference (Δt) of this Mach-Zehnder interferometer should be much longer than the pulse duration. The switch of the device recombines the pulse traveling through the short and the long arms without introducing any loss, which could be replaced by a passive fiber coupler. In our scheme, the photon wave function of one incident circular polarized photon will be split into two parts, transmitted part and the reflected part, by an ordinary nonpolarizing coupler. After interacting with the two parts of the photon wave function are will be recombined by the second ordinary nonpolarizing coupler. Through detecting the photon after the second coupler, we can decide whether the entangled photon pair has been created.

The correspondence between the polarization states and the states obtained by superposition of the two arm ones can be extended. For example, a polarization coupler that separates the basic vertical and horizontal polarization states corresponds to an optical switch between the short and the long pulses. We assume those horizontally polarized pulses with a temporal separation of Δt input into a Mach-Zehnder interferometer. The coherence time of the consecutive pulses is larger than Δt . Then the following time-bin entangled state is created through parametric in MZI.

$$|\Phi\rangle_p = |1,H\rangle_s |1,H\rangle_i + |2,H\rangle_s |2,H\rangle_i \tag{3.20}$$

In the expression $|k,H\rangle$, k is the number of time slots (1 or 2), where denotes the state of polarization [horizontal (H) or vertical (V)], and the subscript identifies whether the state is the signal (s) or the idler (i) state. In Equation (3.20), for simplicity we have omitted an amplitude term that is common to all product states. We employ the same simplification in subsequent equations in this research. This two-photon state with H polarization shown by Figure 3.3 is input into the orthogonal polarization-delay circuit shown schematically in Figure 3.4. The delay circuit consists of a coupler and the difference between the round-trip times of the fiber ring resonator, which is equal to Δt . The polarization controller (PC) is tilted by changing the round trip of the fiber ring is converted into V at the delay circuit output. That is the delay circuits convert; $|k,H\rangle$ to $r|k,H\rangle + t_2 \exp(i\phi)|k+1,V\rangle + rt_2 \exp(i_2\phi)|k+2,H\rangle + r_2 t_2 \exp(i_3\phi)|k+3,V\rangle$ Where t and r is the amplitude transmittances to cross and bar ports in a coupler. Then Equation (3.20) is converted into the polarized state by the delay circuit as

$$
\begin{aligned}
|\Phi\rangle &= [|1,H\rangle_s + \exp(i\phi_s)|2,V\rangle_s] \\
&\times [|1,H\rangle_i + \exp(i\phi_i)|2,V\rangle_i] \\
&+ [|2,H\rangle_s + \exp(i\phi_s)|3,V\rangle_s] \\
&\times [|2,H\rangle_i + \exp(i\phi_i)|2,V\rangle_i] \\
&= [|1,H\rangle_s|1,H\rangle_i + \exp(i\phi_i)|1,H\rangle_s|2,V\rangle_i] \\
&+ \exp(i\phi_s)|2,V\rangle_s|1,H\rangle_i \\
&+ \exp[i(\phi_s + \phi_i)]|2,V\rangle_s|2,V\rangle_i \\
&+ |2,H\rangle_s|2,H\rangle_i + \exp(i\phi_i)|2,H\rangle_s|3,V\rangle_i \\
&+ \exp(i\phi_s)|3,V\rangle_s|2,H\rangle_i \\
&+ \exp[i(\phi_s + \phi_i)]|3,V\rangle_s|3,V\rangle_i
\end{aligned}
\tag{3.21}
$$

By the coincidence counts in the second time slot, we can extract the fourth and fifth terms. As a result, we can obtain the following polarization entangled state as

$$|\Phi\rangle = |2,H\rangle_s |2,H\rangle_i + \exp\left[i(\phi_s + \phi_i)\right] |2,V\rangle_s |2,V\rangle_i \quad (3.22)$$

In this case the fiber acts as a nonlinear medium as a result of the optical Kerr effect. The use of long fiber with a small core is attractive for achieving a high optical intensity and long interaction length. The nonlinearity of the fiber is assumed to be of the Kerr type, i.e., the refractive index is given by

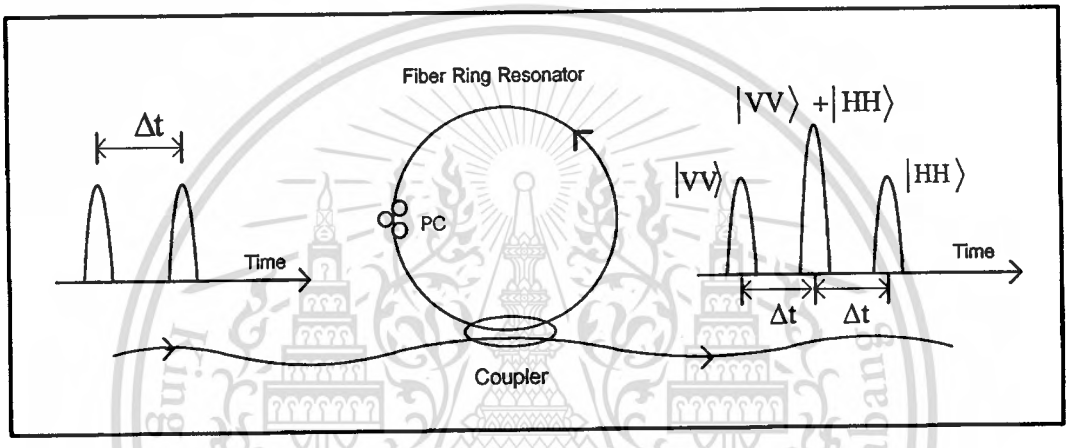

Figure 3.4 A schematic diagram of the polarization delay circuit that uses in the experiment.

$$n = n_0 + n_2 I = n_0 + \frac{n_2 n_0}{2\eta_0}|E|^2 = n_0 + n_2 \frac{P}{S_{eff}} \quad (3.23)$$

where n_0 and n_2 is the linear and nonlinear refractive index of the fiber respectively, and η_0 is the wave impedance in vacuum. I is the instantaneous optical intensity, E the optical electric field, and P the optical power. S_{eff} is the effective mode area depending on the modal field profile in the fiber. All numerical results presented here were calculated for the following values: linear index $n_0 = 1.45$, nonlinear index $n_2 = 3.0 \times 10^{-20}$ m^2/W , and effective mode area $S_{eff} = 50$ μm^2. We assume that the response time of the Kerr effect is much less than the cavity round-trip time. Because of the Kerr nonlinearity of the optical fiber, the strong pulses

acquire an intensity dependent phase shift during propagation. In the fiber ring resonator is arrangement, the weak and the strong propagating pulses acquire different nonlinear phase shifts. When the pulses interfere at the coupler, this relative phase shift realigns the axes of the ellipse. That the fiber optic MZI incorporating a nonlinear fiber optic ring resonator can be used to generate the pulsed polarization-entangled photon pairs, based on the conventional time-bin entanglement arrangement.

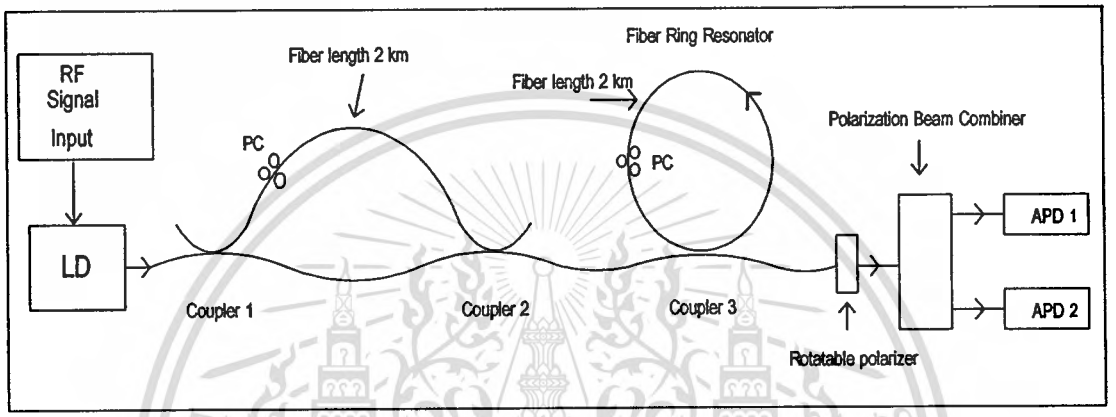

Figure 3.5 The schematic of the experimental setup diagram; LD: Laser diode, PCs: Polarization Controllers, APD: Avalanche Photo detector.

In Figure 3.5 Polarized light pulse is split in to two states via a fiber optic coupler, which randomly propagates in one of the interferometer arms. One of light beams propagates to polarization controller (PC 1) via a fiber optic with 2 km lengths, where the random combination of the entangled pulses is occurred at a second coupler (switch). The optical switch is separate the basic states without losses. The output photons consist of two well-separated pulse energy, which is entangled. Then the output pulses from MZI were launched into the nonlinear fiber ring resonator of the delay circuit. The delay circuit was made of 2-km fiber optic length. This fiber optic length can be designed to precisely adjust the required delay time i.e. Δt , while the change in phase being controlled by using the polarization controller (PC 2). The Kerr type nonlinearly of the effect of light pulses in the optical fiber is occurred while circulating in fiber ring resonator.

Since only the ratio of speed is involved in Snell's law, only the ratio n is determined by measurements of refraction. The definition of the index of refraction of a single medium requires a convention. The convention used is that the index of refraction of a vacuum is exactly 1. Since the speed of light in vacuum is the constant c, the index of refraction n for a substance is given by

$$n = \frac{c}{v} \tag{2.24}$$

where v is the speed of light in the substance. It is important to note that without some definition of global time the physical quantity speed (and thus light-speed) has no definite meaning anyway. Consider an object moving from position A to B. Its speed v is given by the formula

$$v = \frac{S}{t} \tag{2.25}$$

where S is the distance of start to end of fiber optic, t is the time of the start and the finish time in fiber optic. In this research, we used a single mode fiber optic with 2 km lengths, core index $n = 1.45$, $c = 3 \times 10 m/s$, and then the calculation Δt is given by the formula

$$\Delta t = \frac{S}{v} = \frac{2000m}{2.069 \times 10^8 m/s} = 9.67 \times 10^{-6} s$$
$$= 9.67 \mu s$$

then

$$v = \frac{c}{n} = \frac{3 \times 10^8 m/s}{1.45} = 2.069 \times 10^8 m/s$$

The time (Δt) is in Mach Zehnder Interferometer and in fiber optic ring resonator in the same this research.

CHAPTER 4

EXPERIMENTS

The main objective of this study is to understand the experiments of interferometer, photon entangles and time bin entangles, in this chapter, the important experiments are presented.

4.1 Mach Zehnder interferometer

The experimental set up system is shown in Figure 4.1. The quantum approach is used to describe the operating system, where the system can be generally described by either classical or quantum description, where the input light can be a continuous wave, long or short duration pulses. In this work, the orthogonal light signals are formed by linearly polarized light that is modulated by the input inject current into the laser source. Light form modulated laser diode of wavelength with 670 nm, linearly polarized and launched into the interferometer via a beam splitter (BS). One beam was traveled to the mirror M1, and then reflected to the second BS. The another beam is traveled to the mirror M2 and then modulated by the optical modulated unit before entering into the BS, where the combination of light signals i.e. interference signals were detected by the detector, and then was shown on the oscilloscope. The modulated beam was set to offset value using a second controlled polarizer. Variation of optical mediums was employed, and then the corresponding measurement values were recorded. The good optical alignment was taken care to avoid the interferometric noises while the measurement was in progress. When one mode of polarization is launched into the modulator, the coupling mode occurs due to the change of the input orientation angle (i.e. $\Delta\phi$ in equation) causing the change of the optical output power at detector, 1 and 2 respectively.

The experimental set up system for the $LiNbO_3$ modulated is as shown in Figure 4.2. Light form modulated laser diode of wavelength with 670 nm was linearly polarized and launched into the interferometer via a beam splitter (BS1). One beam was traveled to a mirror M1, and then reflected to the second beam splitter (BS2). The another beam is traveled to a mirror M2 and then modulated by $LiNbO_3$ before entering into BS2, where the combination of light signals i.e. interference signals were detected by a pair of compatible detectors and shown on the oscilloscope. The measurement values were initialized to set to offset values by adjusting the second controlled polarizer, and then the corresponding measurement values were recorded.

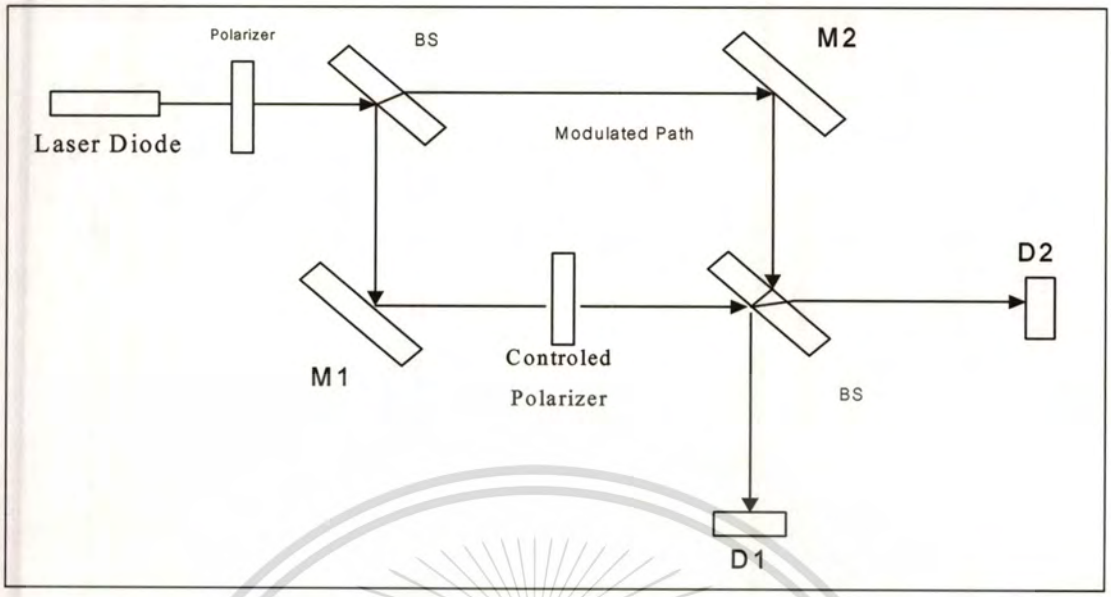

(a)

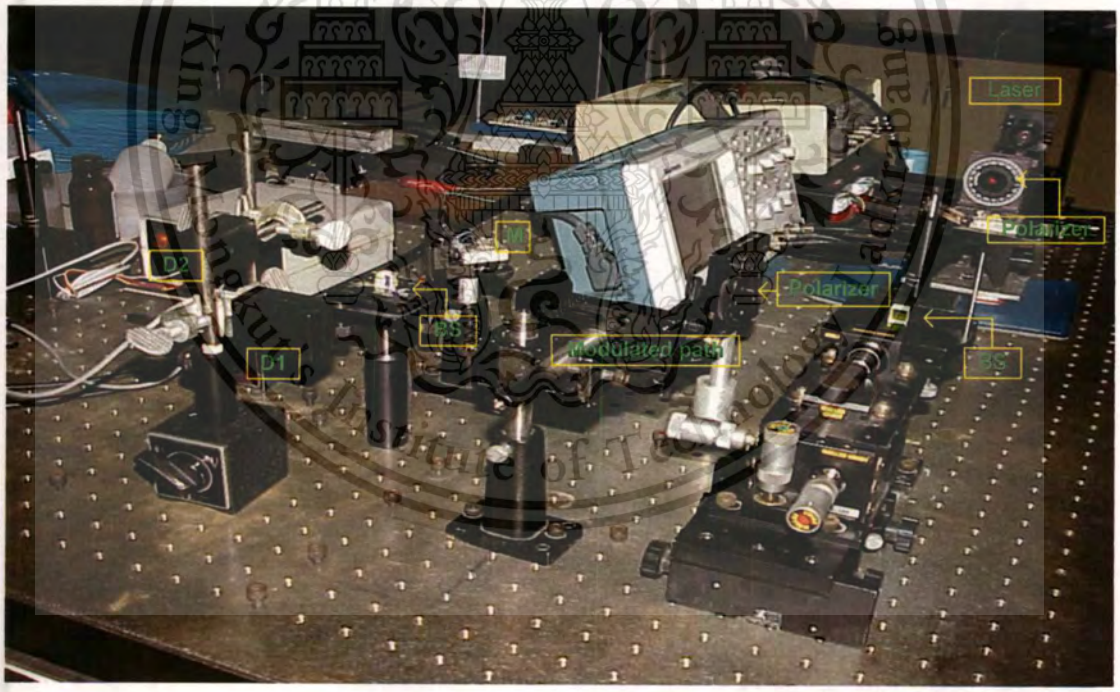

(b)

Figure 4.1 The experimental set up: (a) a schematic diagram, (b) an experimental system. Ms: Mirrors, BS: Beam splitter, Ds: Detectors.

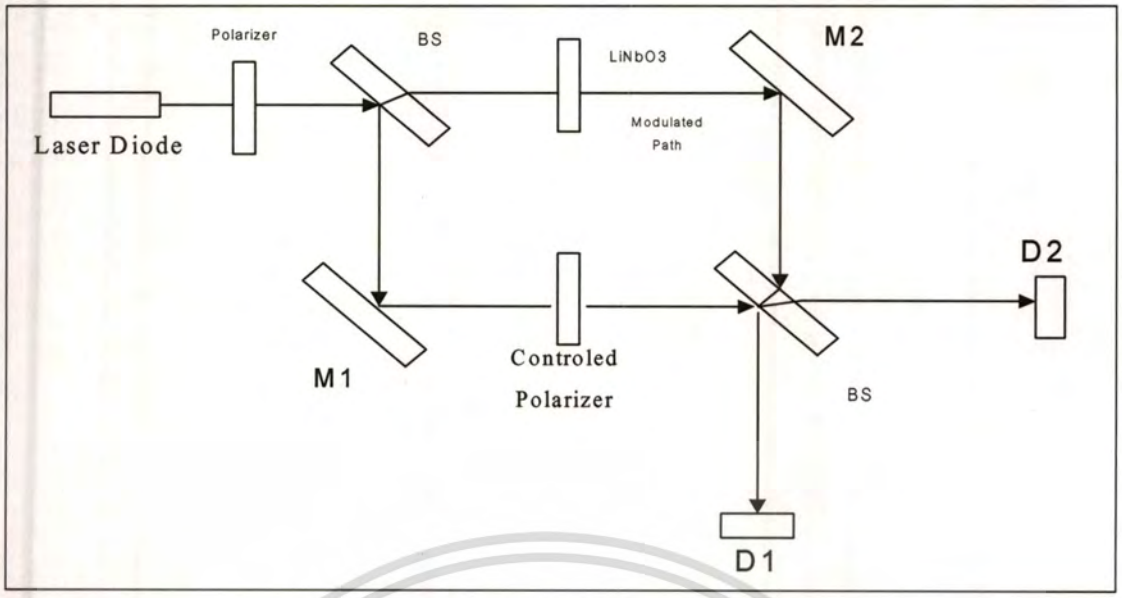

(a)

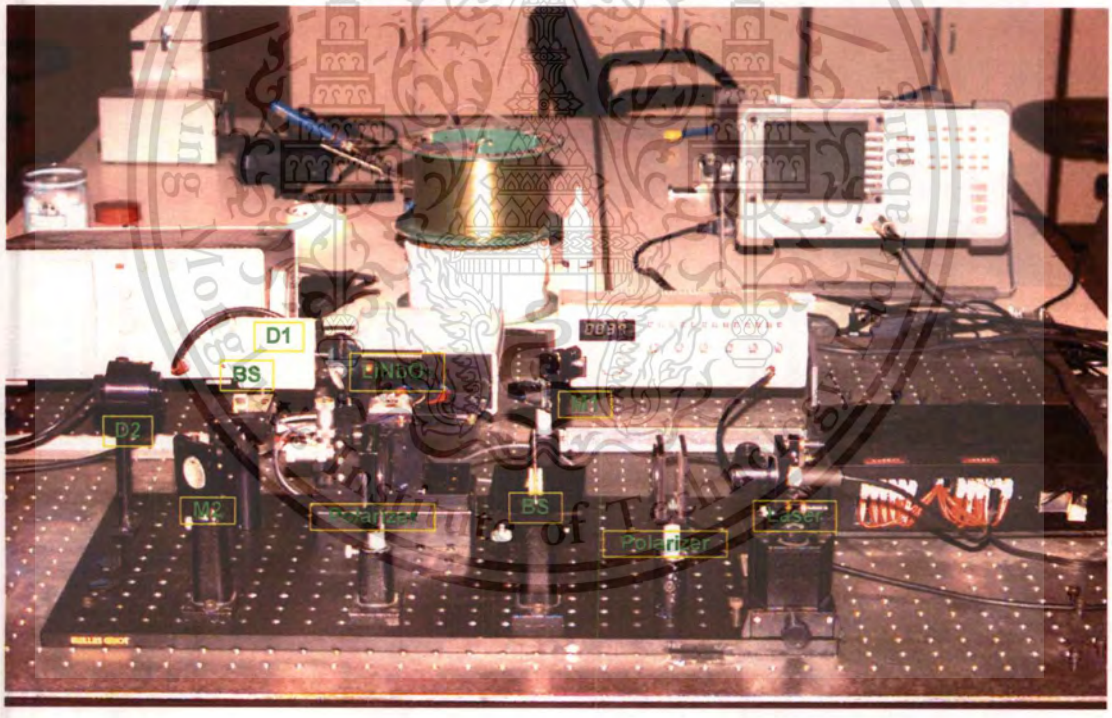

(b)

Figure 4.2 The experimental set up system for the $LiNbO_3$ modulated: (a) a schematic diagram, (b) an experimental system. Ms: Mirrors, BS: Beam splitter, Ds: Detectors.

4.2 Entangled Photons

Figure 4.3 shows a CW laser diode emitter a laser with wavelength of 670 nm, which was linearly polarization right by a controlled polarizer (P1) and randomly launched into a classical MZI via a 50:50 percent beam splitter (BS1). One beam was propagated to mirror M2 then pass to a second beam splitter (BS2). Another beam was propagated through a pumping material i.e. $LiNbO_3$ modulator (LN phase modulator), where the output beam was attenuated and retarded before reflecting at a mirror M1 then combining at a beam splitter BS2. The randomly polarized detected signals and observed and recorded by the two identical detectors and shown on the oscilloscope.

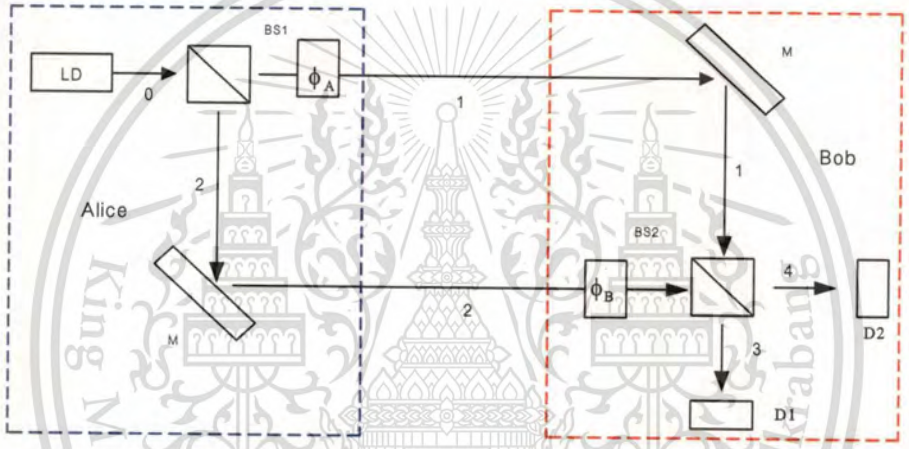

Figure 4.3 Entangle photon scheme bases on a Mach-Zehnder interferometer. LD: Laser diode, BS: Beam splitter, Ms: Mirror, Ds: Detectors.

The system arrangement of the experiment is as shown in Figure 4.3. One mode of the input polarization states traveled into the modulator, where the coupling mode occurred due to the change of the input orientation angle ($\Delta\phi$), which was caused by the change of the optical output power. The largest value of phase ranged from $\Delta\phi = 0$ to 2π . This is different from the one used for a classical interferometer with intensity independent noise. The reason is that the signals and noises disappear at $\Delta\phi = 0$, while the quantum noise more rapidly disappears.

4.3 Time-Bin Entangled Photons

Polarized light from laser diode with wavelength of 1310 nm was modulated with the RF signal at 35 KHz with pulse width of 20 ns, then propagated into MZI as shown in Figure 4.4

Polarized light pulse is split in to two states via a fiber optic coupler (coupler1, 50:50 percent), which randomly propagates in one of the interferometric arms. One of light beams propagates to polarization controller (PC 1) via a fiber optic with 2 km lengths, where the random combination of the entangled pulses is occurred at a second coupler (switch) 50:50 percent. The optical switch is separate the basic states without losses.

The output photons consist of two well-separated pulse energy, which is entangled. Then the output pulses from MZI were launched into the nonlinear fiber ring resonator of the delay circuit. The delay circuit was made of 2-km fiber optic length. This fiber optic length can be designed to precisely adjust the required delay time i.e. Δt ($9.9\mu s$), while the change in phase being controlled by using the polarization controller (PC 2). The Kerr type nonlinearly of the effect of light pulses in the optical fiber is occurred while circulating in fiber ring resonator. Because of the strong pulses acquire an intensity dependent phase shift during propagation in fiber optic ring resonator.

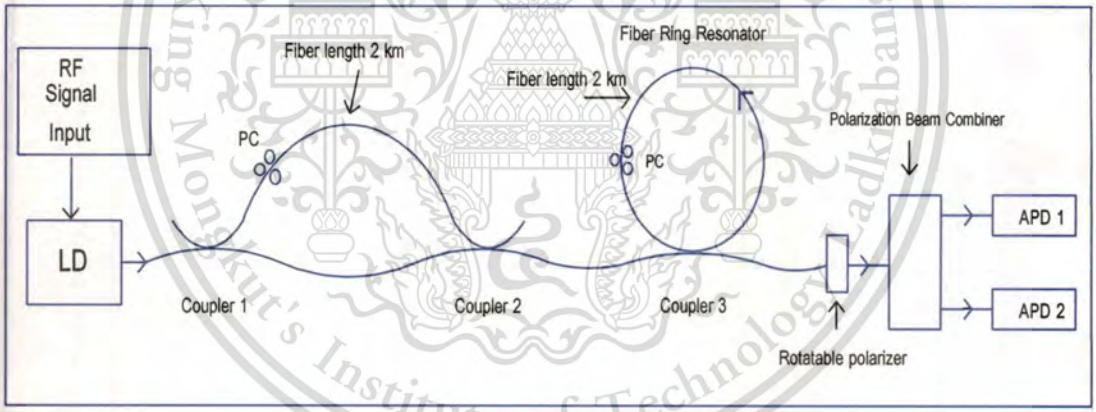

Figure 4.4 The schematic of the experimental setup diagram; LD: Laser diode, PCs: Polarization Controllers, APDs: Avalanche Photo detectors.

The interference of light pulses at a coupler 3 (80:20 percent, 80 percent while circulating in the delay circuit and 20 percent pass to output) introduces the output beam, which is entangled. Due to the polarization states of light pulses are changed and converted while circulating in the delay circuit, where the polarization entangled photon pairs can be generated. To confirm the entangled states the rotation of polarization orientation form 0 to 180^0 can be performed before

launched pulse into the polarization beam combined is in a setup. The polarization angle adjustment device is applied to investigate the orientation and optical output intensity. The entangled photons of the nonlinear fiber optic ring resonator are separated to be the signal and idler photon probability. The polarization angle adjustment device is applied to investigate the orientation and optical output intensity.

CHAPTER 5

RESULTS AND DISCUSSION

The main objective of this chapter is to shown the results of Mach Zehnder interferometer, photon entangles and time bin entangle photon.

5.1 Mach Zehnder interferometer

This is observed and shown in Figure 5.1. The switching characteristics between two channels i.e. detector 1 and detector 2 were observed using a polarizing plate. The polarization orientation angles were varied from 0 to 2π, with the maximum optical outputs is shown as in Figure 5.1, when the input orientation angle were 90, 270 degree, and 135, 315 degree respectively. The signal ambiguity of the two channels was at the orientation angle of 135 and 300 degree. Figure 5.2 (a),(b) shows the phase shifter device characteristic when a length of a single mode sammarian optical fiber of 1 meter with refractive index of 1.52 and polarization maintaining fiber of 1 meter was employed as a modulator. The phase shifter characteristics between two channels were occurred when the orientation angle of 180 degree was presented, which the signals from two channels are at in phase positions differing from the case in Figure 5.1.

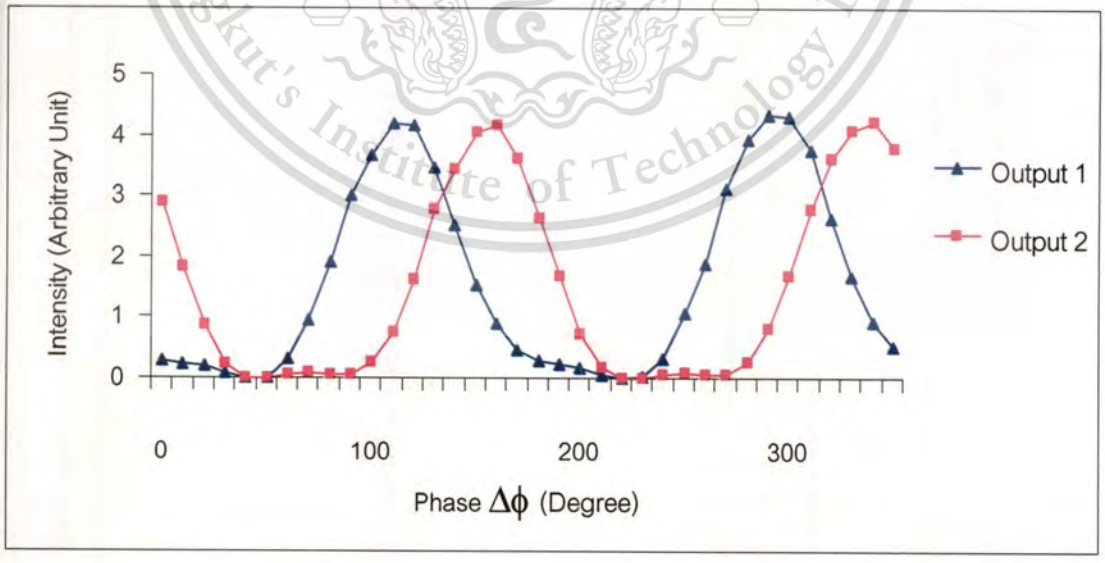

Figure 5.1 Graphs of the results obtained using a polarizer in arm of MZI.

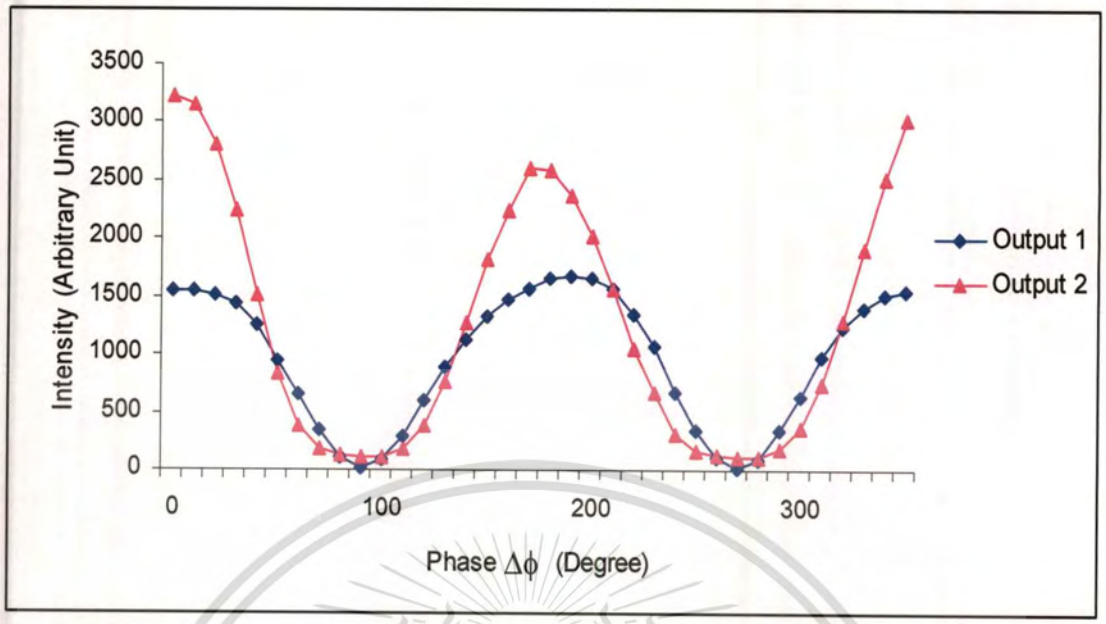

(a)

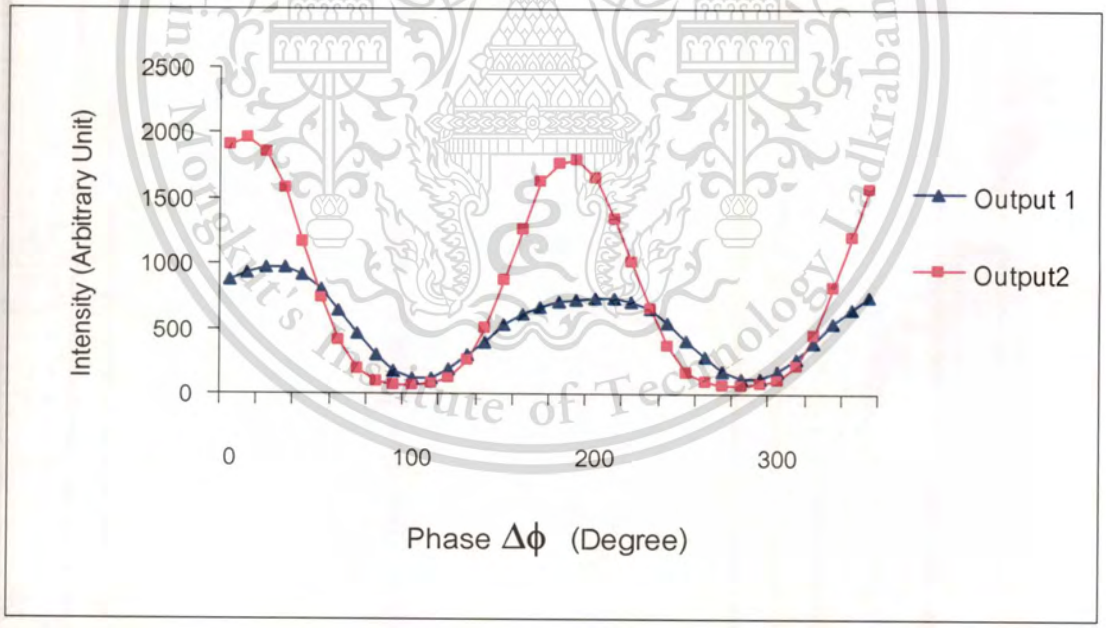

(b)

Figure 5.2 Graphs of the results obtained using; (a) a sammarian opticalfiber, (b) polarization maintaining fiber.

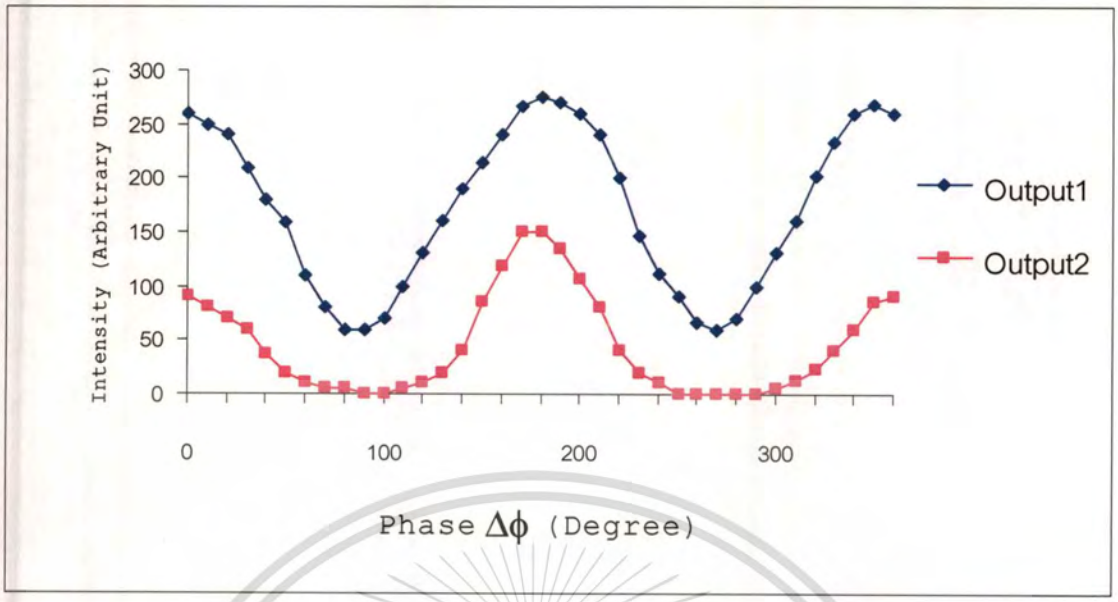

(a)

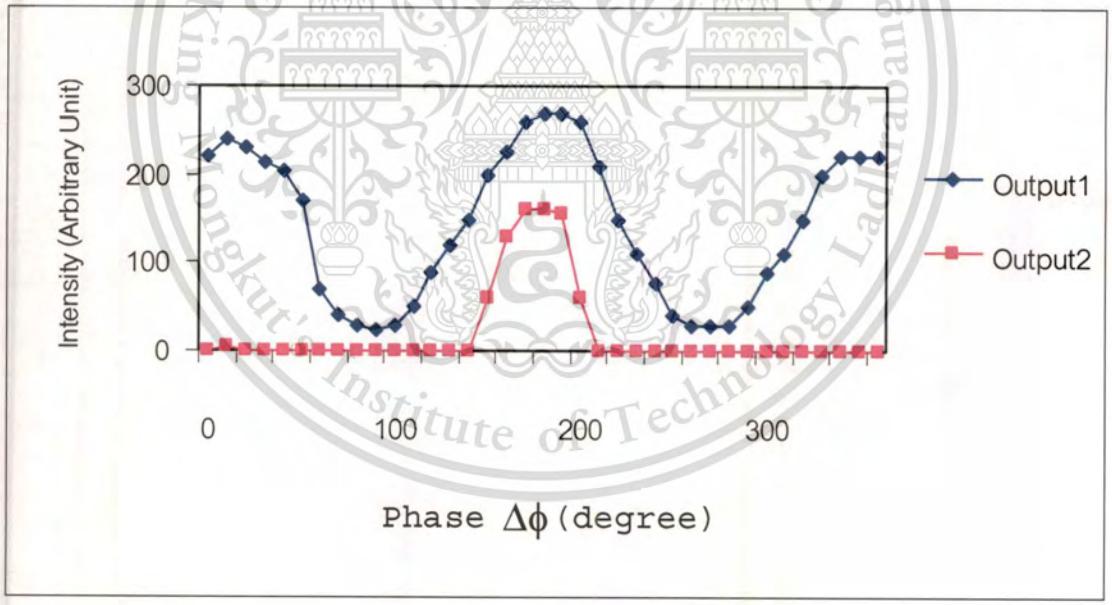

(b)

Figure 5.3 Graphs of the results obtained using; (a) $LiNbO_3$ non-modulate, (b) $LiNbO_3$ modulates.

However, the use of random input transportation and signal output characteristics are the main subject of our continuing work. In practice, the length of a designed fiber can be inline spliced into the optical fiber or device MZI in order to produce the required output signals. Figure 5.3 illustrates graph of the results using $LiNbO_3$ as a modulator with y-cut form, dimension of 1 cm x1cmx 1 mm, refractive index of 2.45 showing the output intensities against the polarization orientation angles. The phase shifter characteristic is observed when the azimuth angle is 45 degree with the S/N and crosstalk respectively. The relationship between output intensities and input polarization angles are plotted. The switching characteristics is occurred when the azimuth angle are at 0, 45 and 135 degree.

5.2 Entangled Photons

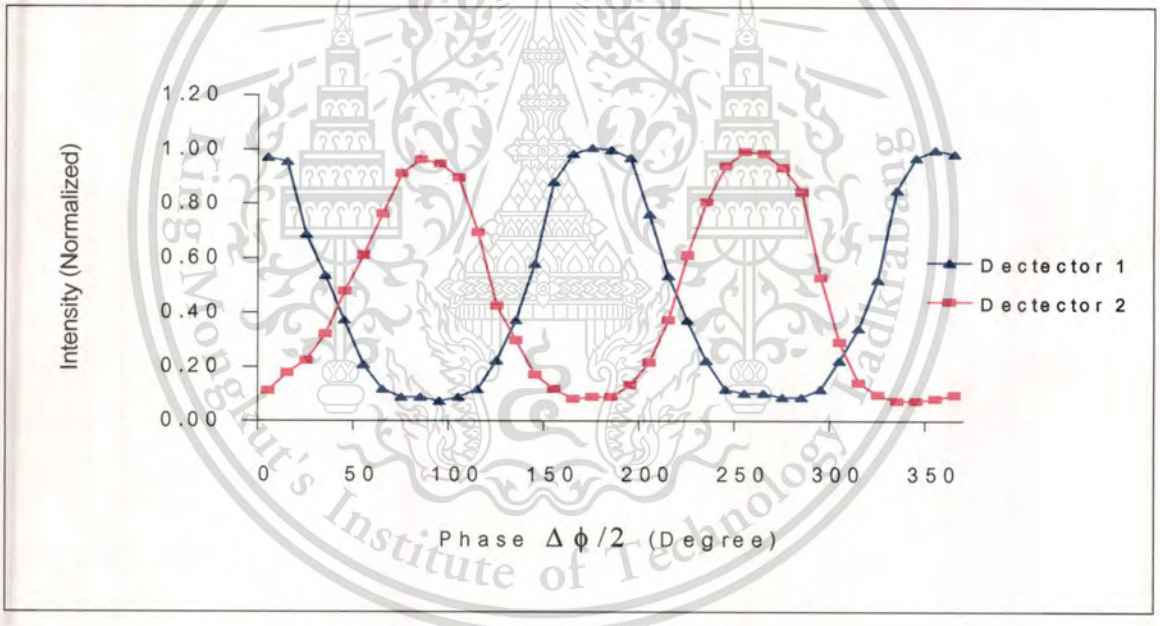

Figure 5.4 Output signal characteristics resulting from the experiment.

The results obtained are shown in Figure 5.4 the output signal characteristics with a linearly polarized light is split and propagated through two arms of the interferometer, one of beam being modulated by a lithium niobate crystal. The signals obtained from both channels are presented as in a phase oscillator with difference signal to noise ratio (S/N). These results are formed by the polarization characteristic of the modulated signals via an external RF signal modulation. Where

the reference detected signal shown in channel 1, relatively to the signal in channel 2, the small effects of the system noise can be neglected. At the detected phase of $(\Delta\phi / 2) = 90^0$, the detected signals at the detectors 1 and 2 are 0 and 1 respectively. Bob can be received the data bits as 0 and 1 from Alice via D1 and D2 respectively. Finally, the entanglement signals can been formed and realized before transmitting via a classical optical system.

5.3 Time Bin entangle Photon

The system of all fiber optic interferometer, it is useful to start with the simple device, which can be entirely understood in terms of classical linear optics. When the photon pulse enter into the device from left-hand side via one end of the coupler, which is assumed that it duration time is shot compared to the length difference of the interferometer arms. In Figure 5.5 show the incoming pulses were split by the first fiber coupler between a short and a longer fiber path, in order to form a temporally separated pulse pair. The path lengths were chosen such that a relative time delay of 9.9 μs (2 km fiber optic length) was obtained between the pair of pulses coupled into the transmission fiber via the second coupler. In this compare the time delay with theoretical are difference 2.3 percent $[((9.9\mu s - 9.67\mu s)/9.9\mu s)\times 100 = 2.3\%]$.

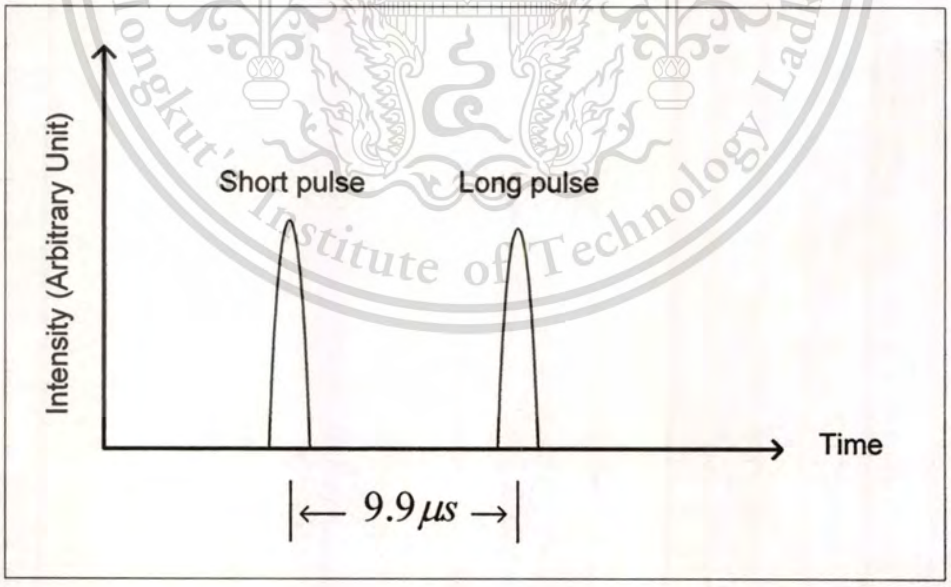

Figure 5.5 The output pulses of the time delay between the pair of pulses after pass MZI.

A phase shifter consisting of which could be varied by polarization control fiber (PC). The output pulses consists of two well-separated pulses which denote them shot and long respectively, which is presented the basis of quantum bit (qubit) space, similarly to the usual vertical $|V\rangle$ and horizontal $|H\rangle$ linear polarization states. The duration time difference (Δt) of this Mach-Zehnder interferometer should be much longer than the pulse duration. The switch of the device recombines the pulse traveling through the short and the long arms. In our scheme, the photon wave function of one incident circular polarized photon will be split into two parts, transmitted part and the reflected part, by an ordinary nonpolarizing coupler. After interacting with the two parts of the photon wave function are will be recombined by the second ordinary nonpolarizing coupler. This two-photon state with H polarization shown by Figure 5.5 is input into the orthogonal polarization-delay circuit. The delay circuit consists of a coupler and the difference between the round-trip times of the fiber ring resonator, which is equal to 9.9 μs and shown by Figure 5.6.

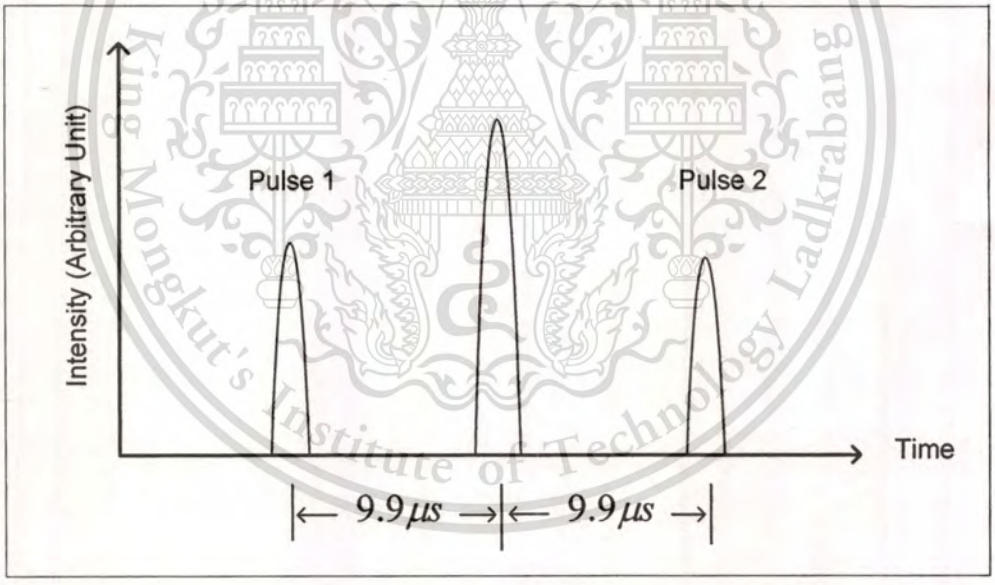

Figure 5.6 The output pulse of the time delay between the pair of pulses after fiber optic ring resonator.

The entangled photons probability is shown in term of the optical output intensity which generated by an all fiber optic system of phase difference $\phi = 180^0$ as shown in Figure 5.7(a), which is in good agreement with the work [7]. Figure 5.7(b) presents the optical intensity at the

output of the polarization output, where the phase difference of the signal at first peak and the delay peak of the nonlinear fiber ring resonator is $\phi = 45^0$. It is shown that the time delay of the signal circulated in the ring resonator is $\Delta t = 9.9\mu s$.

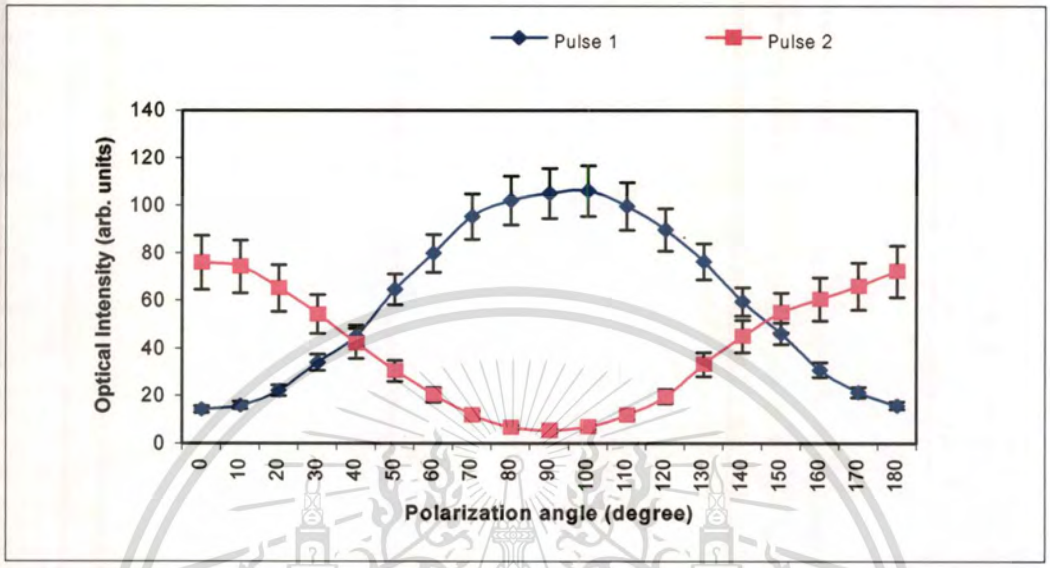

(a)

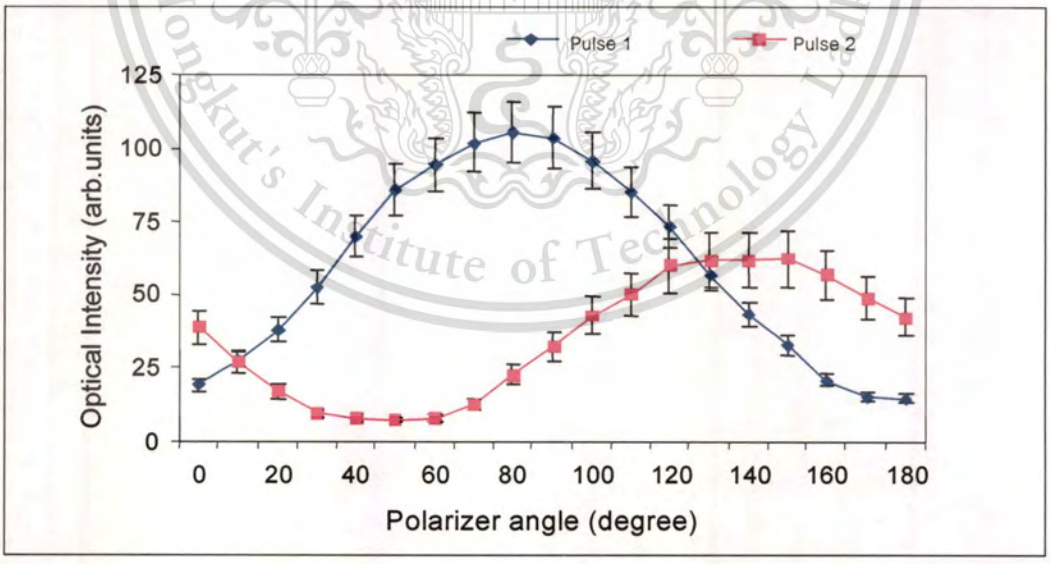

(b)

Figure 5.7 Graphs of the measured optical signals: (a) $\phi = 180^0$, (b) $\phi = 45^0$.

Results obtained have confirmed that the polarization entanglement of the signal and idler photons are realized and occurred. However, to maintain the output of polarization states for long-haul communication may be require the polarization transmission components to link between the sender and receiver before entering into detector, where the sending information is preserved i.e. unchanged. In practice, the use of all fiber optic components is needed to fulfill the use of quantum communication via fiber optic cable, where the perfect security is realized. The other advantage of such a system is that the ease of fiber optic cable connectors can be applied and realized, then the long haul communication link is secured from Eve.

5.4 Discussion

A review of quantum calculations of a Mach Zehnder interferometer has been described. The application for optical signal processing has also been investigated and discussed. Preliminary results using an arrangement of an optical polarizer was shown the possibility of application for the use of other optical modulators. Future work is in program, when the optical modulator such as single mode fiber, Hi bi fiber, nonlinear sammarian fiber and photo elastic material, and also multimode fiber are being used to replace in one path of the instrument. Then the optical signal characteristic can be analyzed for the use of device fabrication design either for optical sensor or communication application.

The modulated technique using Mach-Zehnder interferometer and lithium niobate crystal was proposed for the use of optical and quantum signal processing applications. The optical output signal characteristics can be controlled and analyzed for the use of the device modeling and design, either for optical sensors or communication applications. We have shown that noise of the system using $LiNbO_3$ is neglected comparing to the measurement signals. The good performance of the system together with the small tolerances and the simple arrangement will accomplish new application in future switched wavelength, multiplexing/demultiplexing system and quantum communication applications.

The experimental scheme as shown provides a technique for using the entangled photon and the advantage of using the ultra-short pulse via a quantum channel. It can be used as the referencing data/information to fulfill the required measurement parameters. The interaction between the incident photon and sample will generate the light emission/absorption relationship of the interested physical parameter such as protein. The fluorescence/luminescence of light in the

region of ns can be detected and observed with a high speed detector. The optical filter is required to reject the unwanted background noisy signal. The equivalence scheme using all fiber optics, the fluorescent/luminescent light will be probed and detected by using a detector one (D1) and detector two (D2) for measuring and referencing signals respectively.

We have presented a technique that could be used to generate pulsed polarization-entangled photon pairs by using an orthogonal pulse polarization delay circuit. The system used is based on the system called time bin quantum entanglement, incorporating a nonlinear fiber optic ring resonator for which the response time of the Kerr effect is much less than the cavity round-trip time. The entangled photon pairs were formed by the interference of randomly delayed orthogonal polarized light pulses while circulating in the fiber ring resonator.

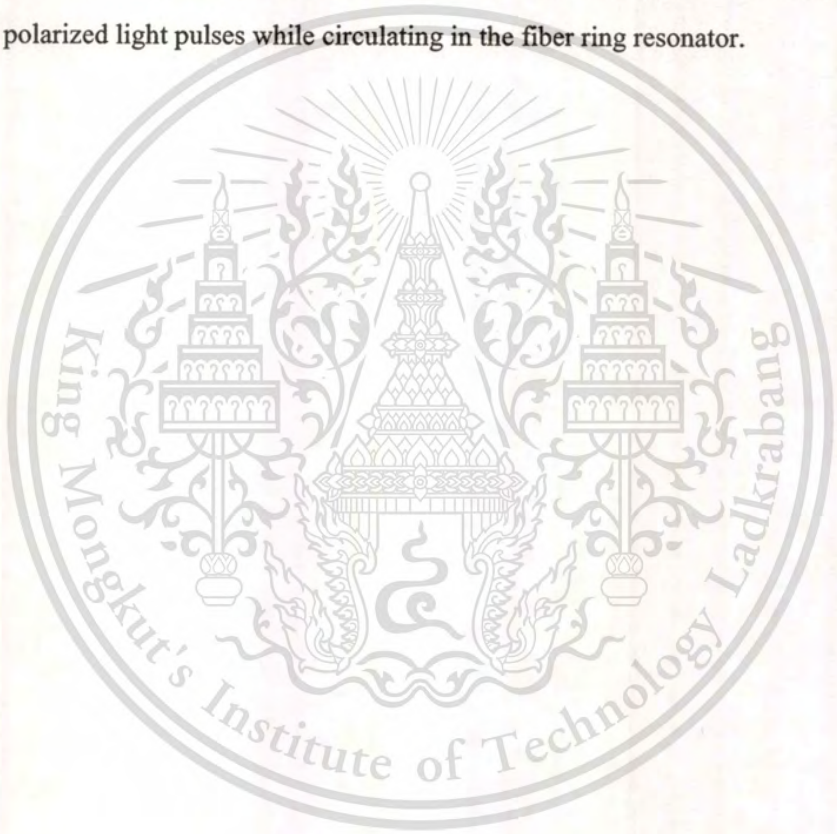

CHAPTER 6

CONCLUSION AND SUGGESTIONS

6.1 Conclusion

1. A review of quantum calculations of the MZI has been described. The applications for optical device and signal processing characterizations have also been investigated and discussed, the preliminary results using optical medium such as polarizer, sammarian nonlinear fiber optic, polarization maintaining fiber and $LiNbO_3$ have shown the possibility of applications such devices for phase shifter switching, demultiplexer and filter. The continuing work is focussed on the use of varieties of optical modulator such as single mode fiber, polarization fiber and some special fibers replacing in one path of the instrument, where the modulated techniques are also employed to produce the appropriate output signals for the applications. When the optical signal characteristics can be analyzed for the use of device modeling and design either for optical sensors or communication applications. While a short pulse can be produced by launching a modulated injected light from a laser diode into a length of a multimode fiber to form the EPR pairs, then the entanglements can be formed and the quantum information can be realized using the classical system.

2. We have assumed the idea of perfectly secured data transmission technique, which it is based on quantum entangled state encryption scheme. Strictly speaking, the set of all possible states sending by Alice to Bob is a set two states corresponding to identical bits, where the two state are horizontal (H) and vertical (V) polarization a single photon. In this application, the idea of an experiment of optical encryption technique can be realized to create top security, for mobile phone up-link converter and communication.

3. We have presented a technique that could be used to generate pulsed polarization-entangled photon pairs by using an orthogonal pulse polarization delay circuit. The system used is based on the system called time bin quantum entanglement, incorporating a nonlinear fiber optic ring resonator for which the response time of the Kerr effect is much less than the cavity round-trip time. The entangled photon pairs were formed by the interference of randomly delayed orthogonal polarized light pulses while circulating in the fiber ring resonator. The obtained entangled photons can be used the in long distance transmission via fiber optic incorporating the classical channel link along the fiber optic. Long haul communication can be realized by using

polarization entanglement pairs to encrypt signals then can be recovered by decrypting the signals at the far end of optical line. This means that the top security using fiber optic link based on quantum cryptography by light is plausible.

6.2 Suggestions

1. For the entangled photons the applications of the phenomena are such as quantum cryptography, quantum teleportation, quantum key and quantum CODEC (code and decode) that they are popularly studied.

2. The obtained entangled photons that can be used the in long distance transmission via fiber optic incorporating the classical channel link along the fiber optic. Long haul communication can be realized by using polarization entanglement pairs to encrypt signals then can be recovered by decrypting the signals at the far end of optical line.

3. In other application, we have pointed out that the advantage of the proposed entangled photon generation system is the remarkably simple optical arrangement, the small device. The proposed system has also shown the potential application for quantum dense coding where the muti-entangled photon pairs are required, which can be implemented via fiber optic link.

REFERENCES

[1] Bennett C.H., Brassard G., Crepeau C., Jozsa R., Peres A. and Wootters W.K. "Teleporting an unknown quantum state via dual classical an Eistein-Podolsky-Rosen.", **Phys. Rev. Lett.**, vol. 70, 1993. Pp. 1895-1899.

[2] Genovese, M. and Novero, C. "Double Entanglement and Quantum Cryptography.", **The European Physical Journal D**, vol. 21, 2002. Pp. 109-113.

[3] Deachapunya, S., Chiangga, S. and Weinfurter, H. "Experimental Quantum Cryptography base on the BB84 Protocol.", **Int. J. Science, KMITL**, vol. 1, 2001. Pp. 80-83.

[4] E. Kreyzig, 1978. **Introductory Functional Analysis with Applications**. New York : John Wiley & Sons.

[5] Ralph T.C., "Mach-Zhender interferometer and the teleporter.", **Phys. Rev. A**, vol. 61, 2000. Pp. 44301-44304.

[6] Mattle K., Weinfurter H., Kwiat P.G. and Zeilinger A. "Dense coding in experimental quantum communication.", **Phys. Rev. Lett., vol.** 76, 1996. Pp. 4656-4659.

[7] H. Weinfurter and Ch. Kurtsiefer, "Entanglement based quantum communication.", **Int. J. Science, KMITL**, vol. 1, 2001. Pp. 35-39.

[8] Suchat S. and Yupapin P.P. "An optical pulse generated using Mach-Zhender interferometer with a $LiNbO_3$ crystal modulator" **Proc. ILLMC Conference, Shanghai, China,** 2001. Pp. 129-132.

[9] Brendel J., Gisin N., Tittel W. and Zbinden H. "Pulsed energy-time entangled twin-photon source for quantum communication.", **Phys. Rev. Lett.**, vol. 82, 1999. Pp. 4656-4659.

[10] Takesue H., Inoue K., Tadanaga O., Nishida Y. and Asobe M. "Generation of pulsed polarization-entangled photon pairs in a 1.55 micrometer band with a periodically poled lithium niobate waveguide and an orthogonal polarization delay circuit.", **Opt. Lett.**, vol. 30, 2005. Pp. 293-295.

[11] Silberhorn C., Lam P.K., Weib O., Konig F., Korolkova N., and Leuchs G. "Generation of continuous variable Einstein-Podolsky-Rosen entanglement via the Kerr nonlinearity in an optical fiber.", **Phys. Rev. Lett.**, vol. 86, 2001. Pp. 4267-4270.

[12] Heebner J.E., Wong V., Schweinsberg A., Boyd R.W. and Jackson D.J. "Optical transmission characteristics of fiber ring resonators.", **IEEE J. of Quantum Electronics,** vol. 40, 2004. Pp. 720-730.

[13] Ogusu K., Shigekuni H., and Yokota Y. "Dynamic transmission properties of a nonlinear fiber ring resonator.", **Opt. Lett.,** vol. 20, no. 22, 1995. Pp. 2288-2290.

[14] Dehlinger D. and Mitchell M.W. "Entangled Photon, Nonlocallity, and Bell Inequallities in the Undergraduate Laboratory.", **Am. J. Phys.**, vol. 70, no.9. 2002. Pp. 903-910.

[15] Bachor, H.A. 1998. **A Guide to Experiments in Quantum Optics.** Weinheim : John Wiley & Sons.

[16] Shin Y., "Entangled Photons.", **IEEE J. of Selected Topics in Quantum Electronic**, vol. 9, no. 6, 2003, pp. 1455-1467.

[17] Leonhardt, U. 1997. **Measuring the Quantum State of Light, Cambridge Studies in Modern Optics.** Cambridge : Cambridge University Press.

[18] Howerton M.M., Moeller R.P., Greenblatt A.S. and Krahenbuhl R. "Fully Packaged, Broad-band $LiNbO_3$ Modulator with Low Drive Voltage.", **IEEE Photonics Techn. Lett.,** vol. 12, no. 7, 2000. Pp. 792-794.

APPENDIX

List of Publication in 2001-2007

[1] P.P. Yupapin, W. Suwanchareon and S. Suchat, "Nonlinearity Penalties and Benefits of Light Traveling in a Fiber Optic Ring Resonator.", **International Journal of Light and Electron Optics**, 2007. (DOI: 10.1016/j.ijleo.2007.07.009)

[2] S. Suchat, W. Khannam and P.P. Yupapin, "Quantum Key Distribution via an Optical Wireless Communication Link for Telephone Network", **Optical Engineering**, vol. 46(10), 2007, Pp.100502. (DOI: 10.1117/1.2786479)

[3] P.P. Yupapin, P. Phiphithirankarn and S. Suchat, "A Quantum CODEC Design via an Optical Add/Drop Multiplexer in a Fiber Optic Network.", **Far East Journal of Electronics and Communications**, vol. 1, no. 2, 2007.

[4] P. P. Yupapin and S. Suchat, "Entangle Photon Generation Using Fiber Optic Mach-Zehnder Interferometer Incorporating Nonlinear Effect in a Fiber Ring Resonator", **Journal of Nanophotonics (JNP)**, vol. 1, 2007, Pp.13504. (DOI: 10.1117/1.2516897)

[5] P.P. Yupapin, S. Suchat and P. Phiphithirankarn, "Time-Bin Entangled Photons using an all Fiber Optic MZI Incorporating a Fiber Ring Resonator", Research Innovation and Vision for the Future, 2007, *IEEE International Conference on RIVF, Vietnam*, 5-9 March 2007. Pp. 181 – 184. Digital Object Identifier 10.1109/RIVF.2007. 369154.

[6] S. Suchat and P.P. Yupapin, "A Non-demolition Measurement of Photon sand Cloning Based on Mach-Zhender Interferometer", *ICMAT'05 (MRS), Singapore*, 2005, Pp. 289-292.

[7] S. Suchat, N. Prasertsang and P.P. Yupapin, A Fiber Optic Remote Sensing for Simultaneous Speed and Load Measurement, *NCOA-1, Bangkok*, 2004, pp. 84 -87.

[8] Suebtarkul Suchat, Preecha P. Yupapin, and Surasak Chiangga, "Quantum entangle photon and applications in communication and measurement", **Songklanakarin J. Sci. Technol.** vol. 26, no. 1, Jan.-Feb. 2004. Pp. 83-91.

[9] S. Suchat and P.P. Yupapin, "An Optical Encryption Technique with Quantum Security Study", **Chiang Mai J. Sci.**, vol. 30(1) 2003. Pp. 27-33.

[10] S. Suchat and P. Yupapin, "A Phase Mask Fiber Grating and Sensing Applications", **Sonklanakarin J. of Sci. and Techn.,** vol. 25, no. 5, 2003. Pp. 615-622.

[11] S. Suchat, S. Paiboon and P.P. Yupapin, "An experiment of optical encryption technique with quantum security for mobile phone up-link converter", *Industrial Technology, 2002. IEEE ICIT '02. Bangkok, Thailand,* vol. 2, 11-14 Dec. 2002. Pp. 1245 – 1248.

[12] S. Suchat ,T. Charnuwong, P.P. Yupapin, and S. Phaiboon, "Generalized Description of Mach – Zehnder Interferometer for Optical Signal Processing Applications" *ISCIT 2001 Conference* , Chiang Mai, Thailand, 14-16 November 2001.

[13] S. Suchat and P.P. Yupapin, "An optical pulse generated using Mach-Zhender interferometer with a $LiNbO_3$ crystal modulator", *Proc. ILLMC Conference*, Shanghai, China, 129-132 (2001).

[14] S. Suchat and P.P. Yupapin, "Optical Phase Shift Study of Optical Devices using MZI for Signal Processing Application", **Int. J. Science, KMITL**, vol. 1, 2001. Pp. 80-83.

[15] S. Suchat, T. Charnuwong and P.P. Yupapin, Generalized Calculation of an Interfermeter with Signal Processing Applications, *Proc. TIP Int. Conf.,* Bangkok, December, 2000.

OE LETTERS

Quantum key distribution via an optical wireless communication link for telephone networks

S. Suchat,[a,b] W. Khunnam,[a] and P. P. Yupapin,[b] MEMBER SPIE
[a]King Mongkut's Institute of Technology Ladkrabang, Advanced Research Center for Photonics, Department of Applied Physics, Faculty of Science, Ladkrabang Bangkok 10520, Thailand
[b]Thammasat University, Department of Physics, Faculty of Science and Technology, Pathumtani 12121, Thailand
E-mail: kypreech@kmitl.ac.th

Abstract. We propose a new system of quantum key distribution via optical wireless communication links, where the required information, especially telephone conversation, can be secured by using a quantum code/decode (CODEC) technique incorporated in the networks. The entangled photons can be encoded into the classical information and then the decoded signal can also be retrieved. The proposed system consists of quantum key generation and uplink and downlink parts that can be implemented in the mobile telephone handset and networks. Such a system and technique show the feasibility of use for a perfectly security telephone networks.
[DOI: 10.1117/1.2786479]

Subject terms: optical wireless; quantum key; perfect security.

Paper 070252LRRR received Mar. 20, 2007; revised manuscript received Jul. 17, 2007; accepted for publication Jul. 23, 2007; published online Oct. 3, 2007.

The mobile telephone has been widely and commonly used for nearly two decades. Because many applications can be provided by a network provider, the demand for use of the mobile phone is large. Furthermore, there are some advantages including a small size, lightweight, and especially, low cost, which means these phones can be applied worldwide. However, there is a serious problem of interception, when perfect security is required by users. Up to now, no system that can secure personal data safely from an eavesdropper has been implemented in telephone networks. Recently, Yupapin and Suchat[1] reported the use of weak light to produce nonlinear behavior of light in a fiber optic ring resonator instead of using a strong light pulse in an ordinary single-mode fiber. Four-wave mixing results from the delayed pulse trains and nonlinear Kerr-type effects in a fiber ring resonator could perform the required entangled states after certain controlled polarization states. Delayed polarization modes via the ring resonator[2] were combined, and the entangled photon states were observed and registered. In practice, the simple design and arrangement of quantum key generation can result in a quantum device for mobile telephone and realistic network use, i.e., the quantum key generation device is now possible in the micrometer scale range. An optical link has shown the potential of being used for long-distance quantum communication, where the transmission of classical and quantum channels are required to transmit via an optical wireless link and where the sender and user can confirm the requested data. Zhou et al.[3] proposed an optical fiber communication system for optical downlink transmission with remote millimeter-wave local-oscillator delivery for intermediate frequency fiber uplink transmission by a wireless transmission of several kilometers. Manderbach et al.[4] have reported on the experimental implementation of Bennett-Brassard 1984 (BB84)-protocol-type quantum key distribution over a 144-km free-space link using weak coherent laser pulses.

In this communication, we propose the concept of an optical wireless communication link for telephone networks. In this concept, we assume that quantum cryptography, quantum teleportation, quantum key and quantum coding and decoding can be implemented using an optical wireless communication link, where the uplink and downlink can be performed and used by a commercial mobile telephone device, where each of the transmitted wavelengths can randomly form the entangled pairs, i.e., the quantum key. The quantum code/decode (CODEC) of the quantum keys can be performed and linked via wireless and optical transmission links. In this application, the idea of an optical encryption technique experiment can be realized to create top-security for mobile telephone uplink and downlink converters and communications. Such a design can also be used with all types of network distributions, where the qubits can be performed and used in the link distributions.

To begin our discussion of this concept, first, we introduce a technique that can be used to create the quantum CODEC. Figure 1 shows[1] a polarization coupler that separates the basic vertical and horizontal polarization states corresponding to an optical switch between short and long pulses. We assume these horizontally polarized pulses with a temporal separation of Δt. The coherence time of the consecutive pulses is larger than Δt. Then the following time-bin state including polarization dispersion is created through a Mach-Zehnder Interferometer (MZI).

$$|\Phi\rangle_p = |1,H\rangle_s|1,H\rangle_i + |2,H\rangle_s|2,H\rangle_i. \quad (1)$$

In the expression of $|k,H\rangle$, k is the number of time slots ($k=1,2$), the state of polarizations are denoted by horizontal (H) or vertical (V), and the subscripts imply the state of the signal (s) or the idler (i). In Eq. (1), for simplicity we omitted an amplitude term that is common to all product states, as done similarly in the subsequent equations in this paper. The two-photon states with H polarization, shown in Eq. (1), are the input into the orthogonal polarization-delay circuit (fiber ring resonator).

The delay circuit consists of a coupler and the difference between the round-trip times of the fiber ring resonator, which is equal to Δt. The polarization controller (PC) is tilted to changing the round trip of the fiber ring, and then converted to V at the delay circuit output. This causes the term $|k,H\rangle$ in Eq. (1) to be converted to the term $r|k,H\rangle + t_2 \exp(i\phi)|k+1,V\rangle + rt_2 \exp(i_2\phi)|k+2,H\rangle + r_2t_2 \exp(i_3\phi)|k+3,V\rangle$. Here t and r are the amplitude transmission coefficients for the throughput and cross-

0091-3286/2007/$25.00 © 2007 SPIE

paths of a coupler. Equation (1) is then converted into the polarized state by the circuit of Fig. 1 as

$$|\Phi\rangle = [|1,H\rangle_s|1,H\rangle_i + \exp(i\phi_i)|1,H\rangle_s|2,V\rangle_i] + \exp(i\phi_s) \times |2,V\rangle_s|1,H\rangle_i + \exp[i(\phi_s+\phi_i)]|2,V\rangle_s|2,V\rangle_i + |2,H\rangle_s|2,H\rangle_i + \exp(i\phi_i)|2,H\rangle_s|3,V\rangle_i + \exp(i\phi_s) \times |3,V\rangle_s|2,H\rangle_i + \exp[i(\phi_s+\phi_i)]|3,V\rangle_s|3,V\rangle_i. \quad (2)$$

By the coincidence of the counts in the second time slot, we can extract the fourth and fifth terms. As a result, we can obtain the following polarization entangled state as

$$|\Phi\rangle = |2,H\rangle_s|2,H\rangle_i + \exp[i(\phi_s+\phi_i)]|2,V\rangle_s|2,V\rangle_i. \quad (3)$$

In the case of a system using weak light input (i.e., without pumping part and component), the fiber acts as a nonlinear medium because of the optical Kerr effect and four-wave mixing in the fiber ring resonator. The use of a long fiber with small core and ring radius is attractive for achieving a high optical intensity and long interaction length. The nonlinear effect that implements this setup is of the four-wave mixing type. In Fig. 1, we proposed a system configuration that the remote access point (RAP) can be required to perform the optical-to-electrical (O/E) and/or electrical-to-optical (E/O) conversion as well as radio frequency (rf) radiating/receiving. The downlink/uplink rf carriers can be feasibly delivered between Alice and Bob. The polarization state from Alice can be maintained by a state registration of polarization state by Bob and consequently he receives the correct polarization state.

Let us first consider the case where the reference photon passes through the path L and the signal photon through the path S, as shown in Fig. 1. In this case, these photons reach the PBC at the same time. As in the parity checking described, the incoming photons in the states $|H\rangle_i|H\rangle_s$ and $|V\rangle_i|V\rangle_s$ (the two photons have different polarizations just before the PBC) result in a two-photon state and a vacuum in the mode X, respectively. On the other hand, the photons in the state $\alpha|V\rangle_i|H\rangle_s+\beta|H\rangle_i|V\rangle_s$ (the two photons have the same polarization just before the PBC) result in one photon in the mode X and one photon in Y, in the state $\alpha|H\rangle_X|H\rangle_Y+\beta|V\rangle_X|V\rangle_Y$. Hence, by counting the number of photons in the mode X, we can discard the cases $|H\rangle_i|H\rangle_s$ and $|V\rangle_i|V\rangle_s$. If Bob detects a photon in $|D\rangle_X$, the two photons are projected onto the state $|D\rangle_X(\alpha|H\rangle_Y+\beta|V\rangle_Y)$. Then Bob obtains the photon in the signal state $\alpha|H\rangle_Y+\beta|V\rangle_Y$.

In a practical communication tasks such as quantum key distribution (QKD), photons in mode Y can be measured on a polarization basis. In this case, one can postselect the event where at least one photon is emitted in each mode X and Y by the twofold coincidence detection. Therefore, the conventional threshold photon detectors, which do not discriminate two or more photons from a single photon, can be used. In the other cases, where the reference photon passes through the path S and/or the signal photon passes through the path L, at least one of the photons should have a different arrival time at detector $|D\rangle_X$ or $|D\rangle_Y$. Hence, we can eliminate the contributions from such cases by discriminating the arrival times of the photons at the detectors $|D\rangle_X$ and $|D\rangle_Y$ by postselection. Any losses in the channels and inefficiencies of the detectors are also discarded by the postselection. A single photon is formed in an MZI that incorporates a fiber optic ring resonator. Each of the entangled pair, which can be clarified by a quantum key between Alice and Bob, where the required memory and speed are realized, can form the correct code, forms the signal. In this application, the idea of the proposed optical encryption technique can be realized to create top security for a mobile telephone uplink converter and communication. The down stream link can be similarly implemented.

We proposed the idea of a new system of the quantum key distribution via an optical wireless communication link for telephone network applications. In practice, a set of all possible states sent by Alice to Bob is a set of two states corresponding to the identical bits, where the two states are horizontal (H) and vertical (V) polarization photons instead of a photon, which is observed as a random orientation. In this application, the idea of the proposed optical encryption technique can be realized to create top security for a mobile telephone uplink converter and communications.

In conclusion, the quantum CODEC can be formed by a fiber optic device, which consists of an MZI incorporated with a fiber optic ring resonator. Then the quantum keys could be distributed in the networks via the optical wireless link, where perfect security can be formed between Alice and Bob without any cheating from Eave. Finally, the classical channel signals can be recovered using the quantum CODEC. The top security information, using a CODEC technique based on quantum cryptography by light, i.e., entangled photons, was discussed and a simple setup demonstrated.

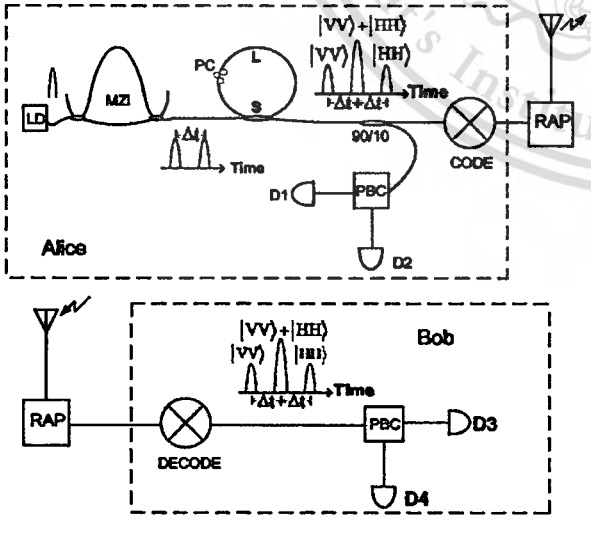

Fig. 1 Schematic diagram of an optical wireless communication link for telephone networks system: PO; polarization control: LD; laser diode; RAP, remote access point; PBC, polarization beam combiner; and D, avalanche photodetector.

Acknowledgments

The authors would like to acknowledge to the Department of Applied Physics, Faculty of Science, King Mongkut's Institute of Technology Ladkrabang (KMITL), Thailand,

for supporting the laboratory facilities. S. Suchat (PhD candidate) would like to acknowledge to the Department of Physics, Faculty of Science and Technology, Thammasat University (TU), Thailand, for some financial support of his study.

References

1. P. P. Yupapin and S. Suchat, "Entangled photon generation using fiber optic Mach-Zehnder interferometer incorporating the nonlinear effect in a fiber ring resonator," *J. Nanophoton.* **1**, 013504 (2007).
2. P. P. Yupapin, P. Saeung, and C. Li, "Characteristics of complementary ring-resonator add/drop filters modeling by using graphical approach," *Opt. Commun.* **272**, 81–86 (2007).
3. M. T. Zhou, J. G. Zhang, A. B. Sharma, Y. Zhang, S. Xiao, and M. Fijise, "Design of millimeter-wave fiber-wireless downlink with remote local-oscillator delivery by using dual-electrode Mach-Zehnder modulators configured for optical single-sideband modulations," *Opt. Commun.* **269**, 69–75 (2007).
4. T. S. Manderbach, H. Weier, M. Furst, R. Ursin, F. Tiefenbacher, T. Scheidl, J. Perdigues, Z. Sodnik, C. Kurtsiefer, J. G. Rarity, A. Zeilinger, and H. Weinfurter, "Experimental demonstration of free space decoy-state quantum key distribution over 144 mm," *Phys. Rev. Lett.* **98**, 010504 (2007).

Journal of Nanophotonics, Vol. 1, 013504 (19 January 2007)

Entangled photon generation using a fiber optic Mach-Zehnder interferometer incorporating the nonlinear effect in a fiber ring resonator

Preecha P. Yupapin and Suebtarkul Suchat
Advanced Research Center for Photonics, Department of Applied Physics,
Faculty of Science, King Mongkut's Institute of Technology Ladkrabang,
Bangkok 10520, Thailand
E-mail: kypreech@kmitl.ac.th or sueb@alpha.tu.ac.th

Abstract. A new system for entangled photon-pair generation using an all-fiber optic scheme consists of a fiber optic Mach-Zehnder interferometer (MZI) incorporating a fiber optic ring resonator. The Kerr nonlinearity effect in the fiber ring resonator is exploited for the generation of two independent squeezed beams. The advantage of such a system is that it requires a simple arrangement without any optical pumping parts or bulky optical components. Polarized light pulse trains are launched randomly into a MZI, and one part of the light is delayed in the longer path. The output pulses from both arms of the MZI enter a fiber optic ring resonator. A polarization controller controls the polarization states of the light pulses while they circulate in the ring resonator. The superposition of the nonlinear light pulses in a fiber optic ring resonator randomly occur. These forms are seen on an avalanche photodetector. The results are in good agreement with previous work.

Keywords: quantum entanglement, quantum optics, fiber optic ring resonators.

1 INTRODUCTION

Quantum information was theoretically well established by Bennett et al. [1]. The proposed scheme was also presented for quantum cryptography by the same authors [2]. This area of research has now been now investigated theoretically [3] or experimentally. It is expected that the implemented systems will have a wide range of applications in the near future. The security of the information is achieved which can be clarified by the link between sender (Alice) and receiver (Bob), without any cheating by Eve. Generally, a single photon can be either a particle or light, where the case of a polarized light pulse having two polarization states corresponding to two spin states of a particle satisfies the quantum entanglement pairs. If the input initial state of the polarized light input is random, the detected signal will be unknown due to the uncertainty principle that the initial information is loose when the output signal is measured.

The applications of the phenomena include quantum cryptography, quantum teleportation, quantum key and quantum CODEC (code and decode). Zellinger et al. [4] have demonstrated that photon can be transported using a classical channel by a Mach-Zehnder interferometer (MZI), where photons in linear or circular polarization states can form the entangled pairs. Quantum cryptography through free space, wireless or optical fiber has been reported. Weinfurter et al. [5] have shown that quantum cryptography can be realized by using a single photon transmission in a light wave channel. Recently he has demonstrated that the four states of polarized light can form quantum cryptography using such a simple arrangement. Suchat and Yupapin [6] have also shown that by using a classical MZI with one arm modulated by a $LiNbO_3$ crystal a single photon can be generated. Brendel et al. [7] have generated pulse polarization entanglement or pulse energy time entanglement by MZI in a delay circuit. Takesue et al. [8] have also shown the same results using a Michelson

Received 11 Oct 2006; accepted 15 Jan 2007; published 19 Jan 2007 [CCC: 19342608/2007/$25.00]

interferometer. Silberhorn et al. [9] have reported on the generation of a continuous variable entanglement using an optical fiber interferometer, where the Kerr nonlinearity in the fiber is exploited for the generation of two independent squeezed beams. The nonlinearity of optical ring resonators has shown great promise for a variety of applications such as optical time delay [10] and optical switching [11].

In this paper, we have made a similar system to that described in Ref. 9 but we use a nonlinear fiber optic ring resonator for the delay and interference signals, which when polarized generates the pulsed polarization-entangled photons. This is a new scheme that uses an all fiber optic system without any optical pumping parts from polarized light pulses. We have demonstrated that an all fiber optic MZI incorporating a nonlinear fiber optic ring resonator can be used to generate pulsed polarization-entangled photon pairs, which are based on the conventional time-bin entanglement arrangement [7].

2 OPERATING PRINCIPLES

A conventional fiber optic Mach-Zehnder interferometer is configured as an intrinsic sensor based on the interference between sensing and reference signals. A standard two-beam interferometer uses a laser diode as a coherent light source.

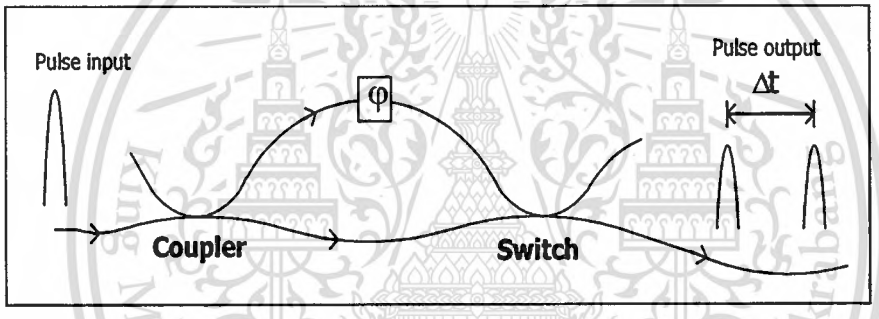

Fig. 1. Schematic of a fiber optic Mach-Zehnder interferometer.

In order to explain the operation of an all fiber optic interferometer, it is useful to start with the simple device shown in Fig. 1, which can be entirely understood in terms of classical linear optics. Let a one-photon pulse enter the device from the left-hand side via one end of the coupler. This pulse is assumed to have a duration which is shot compared to the length difference of the interferometer arms. The output consists of two well-separated pulses, $|short\rangle$ and $|long\rangle$. These form the basis of quantum bit (qubit) space, in a similar way to the usual vertical $|V\rangle$ and horizontal $|H\rangle$ linear polarization states. Hence, the state at the output of our preparation device is formed by $\alpha|short\rangle + \beta|long\rangle$. The relative norm and phase of the coefficients α and β are determined by the coupling ratio (η) of the coupler (beam splitter) and the phase φ of the phase shifter, respectively. Hence, any state of the two-dimensional Hilbert space spanned by the basic states $|short\rangle$ and $|long\rangle$ can be prepared and analyzed. The arm length difference Δt of this Mach-Zehnder interferometer should be much longer than the pulse duration. The switch of the device recombines the pulse traveling through the short and the long arms without introducing any loss. It could be replaced by a passive (50:50)% fiber coupler, and the 50% loss use as an analyzer. The two pulses enter the device from the right.

The switch is synchronized such that the pulse corresponding to the ket $|short\rangle$ takes the long path in the interferometer and vice versa for the other pulse. Hence, at the output (left) of the analyzer, both pulses interfere. Depending on the phase shift and coupling ratio the interference is constructive or destructive and complete or incomplete, respectively, in full analogy with a polarization analyzer.

The correspondence between the polarization states and the states obtained by superposition of the $|short\rangle$ and $|long\rangle$ ones can be extended. For example, a polarization coupler that separates the basic vertical and horizontal polarization states corresponds to an optical switch between the short and the long pulses. We assume that horizontally polarized pulses with a temporal separation of Δt are input into a Mach-Zehnder interferometer. The coherence time of the consecutive pulses is larger than Δt. Then the following time-bin entangled state is created through a parametric system in the MZI:

$$|\Phi\rangle_p = |1,H\rangle_s|1,H\rangle_i + |2,H\rangle_s|2,H\rangle_i \,. \qquad (1)$$

In the expression $|k,H\rangle, k$ is the number of time slots (1 or 2), where A denotes the state of polarization [horizontal (H) or vertical (V)], and the subscript identifies whether the state is the signal (s) or the idler (i) state. In Eq. (1), for simplicity we have omitted an amplitude term that is common to all product states. We employ the same simplification in subsequent equations in this paper. This two-photon state with H polarization shown by Eq. (1) is input into the orthogonal polarization-delay circuit shown schematically in Fig. 2. The delay circuit consists of a coupler and the difference between the round-trip times of the fiber ring resonator [10], which is equal to Δt. The polarization controller (PC) is tilted by changing the round trip of the fiber ring then converted into V at the delay circuit output. That is, the delay circuit converts $|k,H\rangle$ to $r|k,H\rangle + t_2\exp(i\phi)|k+1,V\rangle + rt_2\exp(i_2\phi)|k+2,H\rangle + r_2t_2\exp(i_3\phi)|k+3,V\rangle$, where t and r are the amplitude transmittances to cross and bar ports in a coupler. Then Eq. (1) is converted into an equation for the polarized state by the delay circuit to give

$$\begin{aligned}
|\Phi\rangle &= \left[|1,H\rangle_s + \exp(i\phi_s)|2,V\rangle_s\right] \\
&\quad \times \left[|1,H\rangle_i + \exp(i\phi_i)|2,V\rangle_i\right] \\
&\quad + \left[|2,H\rangle_s + \exp(i\phi_s)|3,V\rangle_s\right] \\
&\quad \times \left[|2,H\rangle_i + \exp(i\phi_i)|2,V\rangle_i\right] \\
&= \left[|1,H\rangle_s|1,H\rangle_i + \exp(i\phi_i)|1,H\rangle_s|2,V\rangle_i\right] \\
&\quad + \exp(i\phi_s)|2,V\rangle_s|1,H\rangle_i \\
&\quad + \exp\left[i(\phi_s+\phi_i)\right]|2,V\rangle_s|2,V\rangle_i + |2,H\rangle_s|2,H\rangle_i \\
&\quad + \exp(i\phi_i)|2,H\rangle_s|3,V\rangle_i + \exp(i\phi_s)|3,V\rangle_s|2,H\rangle_i \\
&\quad + \exp\left[i(\phi_s+\phi_i)\right]|3,V\rangle_s|3,V\rangle_i \,. \qquad (2)
\end{aligned}$$

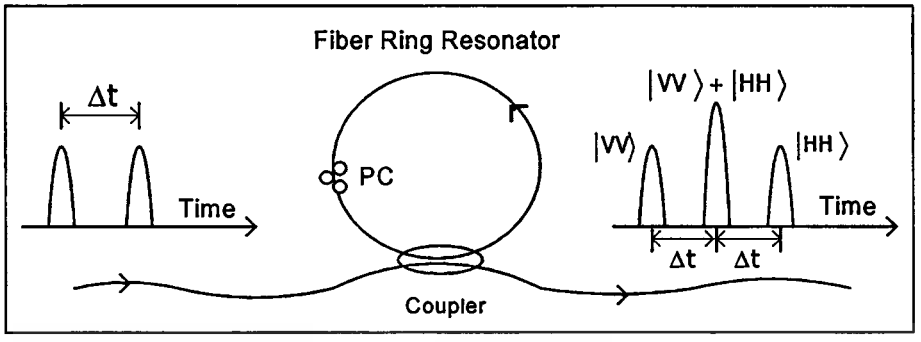

Fig. 2. A schematic diagram of the polarization delay circuit used in the experiment.

By the coincidence counts in the second time slot, we can extract the fourth and fifth terms. As a result, we can obtain the following polarization entangled state as

$$|\Phi\rangle = |2,H\rangle_s|2,H\rangle_i + \exp\left[i(\phi_s+\phi_i)\right]|2,V\rangle_s|2,V\rangle_i \quad . \qquad (3)$$

In this case, the fiber acts as a nonlinear medium because of the optical Kerr effect. The use of a long fiber with a small core is attractive for achieving a high optical intensity and long interaction length. The nonlinearity of the fiber is assumed to be of the Kerr type, and the refractive index is given by [11]

$$n = n_0 + n_2 I = n_0 + \frac{n_2 n_0}{2\eta_0}|E|^2 = n_0 + n_2\frac{P}{S_{eff}} \quad , \qquad (4)$$

where n_0 and n_2 are the linear and nonlinear refractive index of the fiber, respectively, η_0 is the wave impedance in vacuum, I is the instantaneous optical intensity, E is the optical electric field, P is the optical power, and S_{eff} is the effective mode area which depends on the mode field profile of the optical fiber. All numerical results presented here were calculated for the following values: linear refractive index $n_0 = 1.45$, nonlinear refractive index $n_2 = 3.0\times10^{-20}$ m^2/W, and effective mode area $S_{eff} = 50\ \mu m^2$. We assume that the response time of the Kerr effect is much less than the cavity round-trip time. Because of the Kerr nonlinearity of the optical fiber, the strong pulses acquire an intensity dependent phase shift during propagation. In the fiber ring resonator arrangement, the weak and the strong propagating pulses acquire different nonlinear phase shifts. When the pulses interfere at the coupler, this relative phase shift realigns the axes of the ellipse. The fiber optic MZI incorporating a nonlinear fiber optic ring resonator can be used to generate the pulsed polarization-entangled photon pairs, based on the conventional time-bin entanglement arrangement.

3 EXPERIMENT AND RESULTS

Polarized light from a laser diode with wavelength of 1310 nm was modulated with the RF signal at 35 KHz, and a pulse width of 20 ns, and then propagated into MZI as shown in Fig 3. The polarized light pulse is split into two states via a fiber optic coupler which randomly propagates in one of the interferometric arms, and one of the light beams propagates to the polarization controller (PC 1) via a 2-km fiber optic link. The random combination of the entangled pulses occurs at the second coupler, i.e., switch. This is set as an optical switch and

separates the basic states without losses. The output photons consist of two well-separated pulses which are entangled. The output pulses from the MZI are launched into the nonlinear fiber ring resonator of the delay circuit. The delay circuit is made of 2-km fiber optic lengths. This fiber optic length can be designed to obtain precisely the required delay time Δt, while the change in phase is controlled by using the polarization controller (PC 2). The Kerr type nonlinearly effect on light pulses in the optical fiber occurs while the pulses circulate in the fiber ring resonator. Because the pulses are strong, they acquire an intensity dependent phase shift during propagation in the fiber optic ring resonator. The interference of light pulses at coupler 3 introduces the out put signals, which are entangled. The polarization states of the light pulses are changed and converted while circulating in the delay circuit, where the entangled photon pairs can be generated. To confirm the existence of entangled states, the rotation of the polarization orientation from 0 to 180 deg can be performed before launching the pulse into the polarization beam combined setup. The polarization angle adjusting device is applied to investigate the orientation and optical output intensity. The entangled photons of the nonlinear fiber optic ring resonator are separated into signal and idler photon probability.

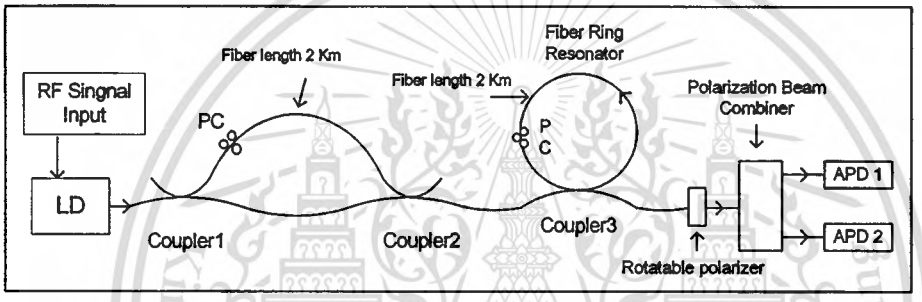

Fig. 3. The schematic of the experimental setup diagram; LD: laser diode, PCs: polarization controllers, APD: avalanche photodetector.

The entangled photons probability is shown in term of the optical output intensity which is generated by using an all fiber optic system of phase difference $\phi = 0°$ as shown in Fig. 4(a), which is in good agreement with the previous work [7]. Figure 4(b) presents the optical intensity at the output of the polarization output, where the phase difference of the signal at first peak and the delay peak of the nonlinear fiber ring resonator is $\phi = 45°$. It is shown that the time delay of the signal circulated in the ring resonator is $\Delta t = 9.9\mu s$. Results obtained have confirmed that the polarization entanglement of the signal and idler photons are realized. However, maintaining the output of the polarization states for long-haul communication may require the polarization transmission components to link between the sender and receiver before entering into the detector, where the sending information is preserved. In practice, the use of all fiber optic components is needed for quantum communication via fiber optic cable, where perfect security is required. The other advantage of such a system is that it is easy to make a long haul communication link which is secured from Eve.

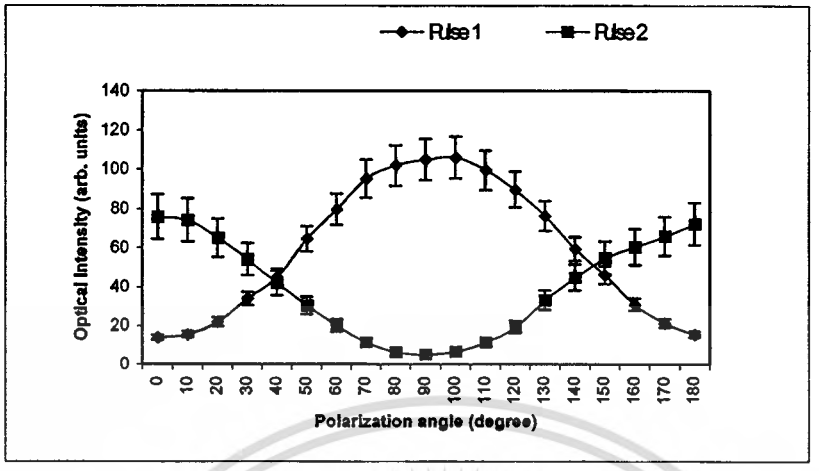

(a)

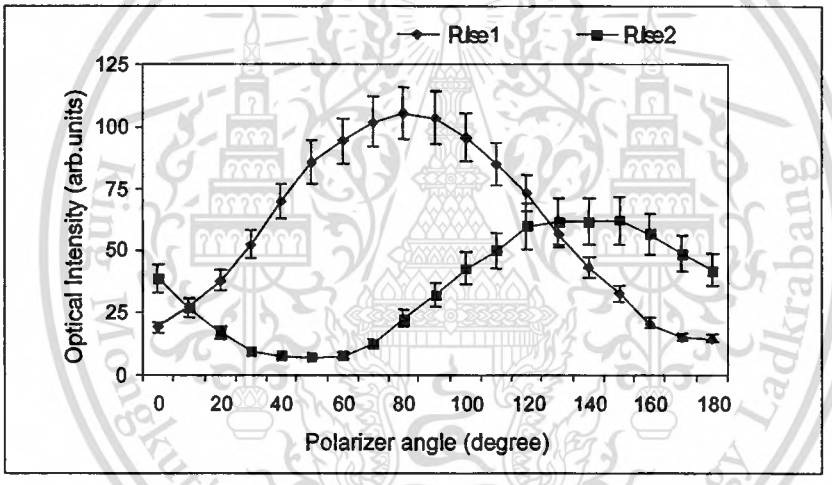

(b)

Fig. 4. Graphs of the measured optical signals: (a) $\phi = 0°$, (b) $\phi = 45°$.

4 CONCLUDING REMARKS

We have presented a technique that could be used to generate pulsed polarization-entangled photon pairs by using an orthogonal pulse polarization delay circuit. The system used is based on the system called time-bin quantum entanglement, incorporating a nonlinear fiber optic ring resonator for which the response time of the Kerr effect is much less than the cavity round-trip time. The entangled photon pairs were formed by the interference of randomly delayed orthogonal polarized light pulses while circulating in the fiber ring resonator.

In conclusion, the obtained entangled photons can be used in long distance transmission via fiber optics incorporating the classical channel link along the fiber optics. Long haul communication can be realized by using polarization entanglement pairs to encrypt signals then can be recovered by decrypting the signals at the far end of optical line. This means that top security using a fiber optic link based on quantum cryptography by light is plausible.

Acknowledgments

The authors acknowledge the Department of Applied Physics, Faculty of Science, King Mongkut's Institute of Technology, Ladkrabang (KMITL), Thailand, for supporting the laboratory facilities. S. Suchat (Ph.D. candidate) acknowledges the National Science and Technology Development Agency (NSTDA) and Department of Physics, Faculty of Science and Technology, Thammasat University, Thailand for some financial support of his study. The authors thank Prof. M. Allen of Mahidol University, Thailand for his useful comments and proofreading this manuscript.

References

[1] C.H. Bennett, G. Brassard, C. Crepeau, R. Jozsa, A. Peres, and W.K. Wootters, "Teleporting an unknown quantum state via dual classical and Einstein-Podolsky-Rosen channels", *Phys. Rev. Lett.* **70**, 1895-1899 (1993). [doi:10.1103/PhysRev Lett.70.1895]

[2] T.C. Ralph, "Mach-Zehnder interferometer and the teleporter", *Phys. Rev. A* **61**, 44301-44304 (2000). [doi:10.1103/PhysRevA.61.044301]

[3] E. Kreyzig, *Introductory Functional Analysis with Applications*, John Wiley & Sons, New York (1978).

[4] K. Mattle, H. Weinfurter, P. G. Kwiat, and A. Zeilinger, "Dense coding in experimental quantum communication", *Phys. Rev. Lett.* **76**, 4656-4659 (1996). [doi: 10.1103/PhysRevLett.76.4656.044301]

[5] H. Weinfurter and Ch. Kurtsiefer, "Entanglement based quantum communication", *KMITL Sci. J.* **1**, 35-39 (2001).

[6] S. Suchat and P.P. Yupapin, "An optical pulse generated using Mach-Zehnder interferometer with a $LiNbO_3$ crystal modulator", *Proc. ILLMC Conference*, Shanghai, China, 129-132 (2001).

[7] J. Brendel, N. Gisin, W. Tittel and H. Zbinden, "Pulsed energy-time entangled twin-photon source for quantum communication", *Phys. Rev. Lett.* **82**, 4656-4659 (1999). [doi:10.1103/PhysRevLett.82.2594]

[8] H. Takesue, K. Inoue, O. Tadanaga, Y. Nishida and M. Asobe, "Generation of pulsed polarization-entangled photon pairs in a 1.55 micrometer band with a periodically poled lithium niobate waveguide and an orthogonal polarization delay circuit", *Opt. Lett.* **30**, 293-295 (2005). [doi:10.1364/OL.30.000293]

[9] C. Silberhorn, P.K. Lam, O. Weib, F. Konig, N. Korolkova, and G. Leuchs, "Generation of continuous variable Einstein-Podolsky-Rosen entanglement via the Kerr nonlinearity in an optical fiber", *Phys. Rev. Lett.* **86**, 4267-4270 (2001). [doi:10. 1103/PhysRevLett.86.4267]

[10] J.E. Heebner, V. Wong, A. Schweinsberg, R.W. Boyd and D.J. Jackson, "Optical transmission characteristics of fiber ring resonators", *IEEE J. Quantum Electron.* **40**, 720-730 (2004).

[11] K. Ogusu, H. Shigekuni, and Yokot,, "Dynamic transmission properties of a nonlinear fiber ring resonator", *Opt. Lett.* **20**, 2288-2290 (1995).

Preecha P. Yupapin received his Ph.D. in electrical engineering from City University, London in 1993. He is a professor in applied physics in the Advanced Research Center for Photonics, Department of Applied Physics, Faculty of Science, King Mongkut's Institute of Technology Ladkrabang, Bangkok, Thailand. His research interests are in optical sensors, optical metrology, optical communication, optical signal processing, and quantum information. Professor Yupapin is a member of the Thai Institute of Physics (TIP) and SPIE, and is the president of the Thailand chapter of the Optical Society of America (OSA-Thailand).

Suebtarkul Suchat received his B.Sc. in physics from Ramkamhaeng University, Bangkok, and received his M.Sc. in applied physics from Faculty of Science, King Mongkut's Institute of Technology Ladkrabang, Bangkok, Thailand. He is currently a Ph.D. student in the Department of Applied Physics, Faculty of Science, King Mongkut's Institute of Technology Ladkrabang, Bangkok, Thailand.

XML:ver:5.0.1
5 jena
IJLEO : 50447
Prod.Type:FTP
pp.1–6(col.fig.:2–5,7)
ED:JyothiG
PAGN:santhamma SCAN:
60

ARTICLE IN PRESS

Available online at www.sciencedirect.com
ScienceDirect

ELSEVIER

Optik ▮ (▮▮▮▮) ▮▮▮–▮▮▮

Optik Optics

www.elsevier.de/ijleo

Nonlinearity penalties and benefits of light traveling in a fiber optic ring resonator

P.P. Yupapin*, W. Suwanchareon, S. Suchat

Research and Development Center for Science, Department of Applied Physics, Faculty of Science, King Mongkut's Institute of Technology Ladkrabang, Bangkok 10520, Thailand

Received 19 March 2007; accepted 15 July 2007

Abstract

The nonlinearity properties of light traveling in a fiber optic ring resonator (FORR) are presented. The nonlinearity penalties suffering from Kerr effects and four-wave mixing nonlinear types including bistability, chaos and bifurcation are investigated. The advantages of the nonlinearity penalties including photon correlation, optical switching and information security using chaotic signals are also discussed. The obtained results have shown that the parameters of FORR can be changed, and thus the penalties of the nonlinear effects have shown the potential of using for some applications.

Keywords: Nonlinearity penalty; Fiber ring resonator; Nonlinearity benefit

1. Introduction

Nonlinear effects of light traveling in a fiber optic ring resonator (FORR) have become the area of growing interest for all-optical signal processing and communication. Theoretical studies of all-fiber systems have been based on ring cavities [1,2], Fabry–Perot cavities [3] and nonlinear optical loop mirror with feedback [4,5]. It has been pointed out recently that the majority of the analysis on the optical bistable behavior of these fiber systems has been undertaken using the so-called graphical method developed by Felber and Marburger [6,7], who examined the optical bistability of the optical Fabry–Perot system containing a Kerr medium. Bischofberger and Shen [8] have reported the study of dynamic transmission properties of a nonlinear fiber ring resonator. One type of dynamics, found by Ikeda [9,11], is a route to optical chaos through period doubling in a unidirectional ring cavity containing a Kerr medium. Ikeda applied an iterative method [9] and linear stability analysis [9] in the initial examination of the ring system. These approaches highlighted the inability of the graphical method to direct the regions of unstable behavior. Examination of these instabilities reveals two necessary conditions for their existence: (i) the relaxation time of the nonlinearity needs to be shorter than the ring cavity round trip time and (ii) the phase shift of the electric field in passing around the ring resonator has to be greater than unity. Since it is usual to assume that the Kerr nonlinearity of an optical fiber has an instantaneous relaxation time [10], then it follows that nonlinear optical fiber will satisfy the above conditions, provided the length of the fiber is long enough, or the optical power within the fiber is high enough, or both, to induce the necessary phase shift.

*Corresponding author.
E-mail address: kypreech@kmitl.ac.th (P.P. Yupapin).

0030-4026/$ - see front matter © 2007 Elsevier GmbH. All rights reserved.
doi:10.1016/j.ijleo.2007.07.009

Please cite this article as: P.P. Yupapin, et al., Nonlinearity penalties and benefits of light traveling in a fiber optic ring..., Opt. Int. J. Light Electron. Opt. (2007), doi:10.1016/j.ijleo.2007.07.009

Nakatsuka et al. [10] showed this to be the case, observing bifurcations leading to chaos in a fiber ring resonator. Most of the previous works have analyzed clearly in detail; however, they have not shown the details of the advantages of the nonlinearity penalties. In this paper, we present in some detail the effects of nonlinearity of light pulses traveling in a FORR. There are two types of nonlinear effects proposed in this paper: firstly, the nonlinear effects occurs when the intense light pulses are input into the FORR, which is known as Kerr-type nonlinear effects. While the other type is the four-wave mixing type, which occurs when the weak input light is input into the FORR. However, the ring radius can be varied to obtain the Kerr nonlinearity type in this case. The applications of the nonlinearity penalties including the entangled photon source generation, optical switching and signal security are discussed in detail.

2. Nonlinearities

The architecture of a nonlinear FORR is illustrated in Fig. 1, which is constructed by a single fiber coupler and one ring resonator. We assume that the nonlinearity of the fiber ring is of the Kerr-type, i.e., the refractive index is given by

$$n = n_0 + n_2 I = n_0 + \left(\frac{n_2}{A_{\text{eff}}}\right) P, \tag{1}$$

where n_0 and n_2 are the linear and nonlinear refractive indexes, respectively. I and P are the optical intensity and optical field power, respectively. The effective mode core area of the fiber is A_{eff}.

The input light is launched in port 3 and the output emerges from port 4. It is worth noting that such a device has no reflected wave or no cross-phase modulation occurring at the fiber coupler. Ports 1 and 2 are connected with a fiber having a nonlinear refractive index n_2 and a linear absorption coefficient α. The fiber coupler has an intensity-coupling coefficient κ, and γ is a coupling loss for the field amplitude. We assume

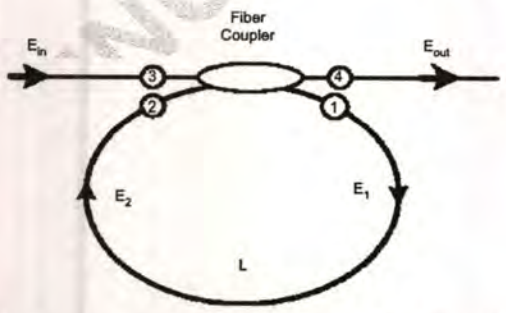

Fig. 1. Schematic diagram of the FORR with a single fiber coupler and one ring resonator.

hereafter (without loss of generality) that the optical fiber ring is on resonance for the operating wavelength in the limit of vanishing incident power, i.e. in the linear case. In addition, we assume that the fiber coupler acts as a point device. The fiber coupler is assumed to be reciprocal and the transmission coefficients for the fields are

$$t_{34} = t_{21} = (1-\gamma)\sqrt{1-\kappa}, \quad t_{31} = t_{24} = \mathrm{j}(1-\gamma)\sqrt{\kappa},$$
$$t_{32} = t_{41} = 0. \tag{2}$$

The following relations of the electric fields arise from Eq. (1):

$$E_1 = t_{31}E_{\text{in}} + t_{21}E_2, \tag{3a}$$

$$E_{\text{out}} = t_{34}E_{\text{in}} + t_{24}E_2. \tag{3b}$$

The relation between the electric fields E_1 and E_2, in the stationary state, can be obtained from the nonlinear propagation equation:

$$\frac{\partial E}{\partial z} = \mathrm{j}\frac{2\pi n_2}{\lambda}|E|^2 E - \frac{1}{2}\alpha E. \tag{4}$$

Integrating Eq. (4) directly, we can thus obtain the following relation:

$$E_2 = E_1\tau\exp(-\mathrm{j}\phi) = E_1\tau\exp\{-\mathrm{j}(\phi_0 + \phi_{\text{NL}})\}, \tag{5}$$

where $\phi_0 = kLn_0$ and $\phi_{\text{NL}} = kLn_2|E_1|^2$ are the linear and nonlinear phase shift, $k = 2\pi/\lambda$ is the wave propagation number in a vacuum and L is the fiber ring resonator length. $\tau = \exp(-\alpha L/2)$ is a one round trip loss in FORR.

It was discovered in 1979 that the nonlinear response of a ring resonator can initiate a period-doubling route to optical chaos. The basic idea consists of recognizing that the dynamics in FORR correspond to that of a nonlinear map round trip inside the FORR. Mathematically, from Eqs. (3) and (5) the map can be written as

$$E_1(t) = \mathrm{j}(1-\gamma)\sqrt{\kappa}E_{\text{in}} + (1-\gamma)\sqrt{1-\kappa}\tau E_1(t-t_R)\exp(-\mathrm{j}\phi). \tag{6}$$

$$E_{n+1} = \mathrm{j}(1-\gamma)\sqrt{\kappa}E_{\text{in}} + (1-\gamma)\sqrt{1-\kappa}\tau E_n\exp(-\mathrm{j}\phi), \tag{7}$$

where the subscript "n" denotes the number of round trips inside the FORR. Using Eq. (7), the nonlinear map can be iterated for a given value of the input power P_{in} ($\alpha|E_{\text{in}}|^2$). The results show that the output of the FORR can become time dependent even for a CW input. Moreover, the output becomes chaotic following a period-doubling route in a certain range of input parameters.

The nonlinear phenomenon of optical bistability has been studied in nonfiber resonators since 1976 by placing the nonlinear medium inside a cavity formed by using multiple mirrors [7–9]. The single-mode fiber was used in 1983 as the nonlinear medium inside a ring

Please cite this article as: P.P. Yupapin, et al., Nonlinearity penalties and benefits of light traveling in a fiber optic ring..., Opt. Int. J. Light Electron. Opt. (2007), doi:10.1016/j.ijleo.2007.07.009

cavity [10]. Since then, the study of nonlinear phenomena in fiber ring resonators has remained a topic of considerable interest. Consider at steady state, from Eq. (6), we have

$$E_1 = \mathrm{j}(1-\gamma)\sqrt{\kappa}E_{\mathrm{in}} + (1-\gamma)\sqrt{1-\kappa}\tau\,\exp(\mathrm{j}\phi)E_1, \quad (8)$$

while the output field at steady state as

$$E_{\mathrm{out}} = (1-\gamma)E_{\mathrm{in}}\left[\sqrt{1-\kappa} - \frac{(1-\gamma)\kappa\tau\,\exp(\mathrm{j}\phi)}{1-(1-\gamma)\sqrt{1-\kappa}\tau\,\exp(\mathrm{j}\phi)}\right]. \quad (9)$$

Thus the normalized light field from Eq. (9) can be expressed as

$$\left|\frac{E_{\mathrm{out}}}{E_{\mathrm{in}}}\right|^2 = (1-\gamma)^2\left[1 - \frac{\kappa[1-(1-\gamma)^2\tau^2]}{1+(1-\gamma)^2(1-\kappa)\tau - 2(1-\gamma)\sqrt{1-\kappa}\tau\cos\phi}\right]. \quad (10)$$

Eqs. (7) and (10) are mathematical relations used for characterizing nonlinear effects such as bifurcation, chaos and optical bistability.

3. Penalties and benefits

The parameters of the simulation results were set as follows: input light with design wavelength $\lambda = 1.55\,\mu\mathrm{m}$, $n_0 = 1.45$, $A_{\mathrm{eff}} = 30\,\mu\mathrm{m}^2$, $\alpha = 0.02\,\mathrm{dB/km}$, $\gamma = 0.1$ and $L = 80\,\mathrm{m}$ and the power coupling coefficient $\kappa = 0.9$. Here, the constant linear phase term is neglected $\phi_0 = 0$. In this study, the plot of 10,000 iterations of round trips inside the optical fiber ring, in Fig. 2(a), shows the curve of output power as a function of the number of ring passes in FORR. The maximum output power resulting from pumping the CW envelope is approximately 140 W. However, to meet the realistic application, the smaller ring length with lower input power than the parameters in Fig. 2(a) are introduced as the result shown in Fig. 2(b). The parameters of the system used were fixed with $\lambda = 1.55\,\mu\mathrm{m}$, $n_0 = 3.37$, $n_2 = 2.69 \times 10^{-17}\,\mathrm{m}^2/\mathrm{W}$, $A_{\mathrm{eff}} = 0.25\,\mu\mathrm{m}^2$, $\alpha = 0.2\,\mathrm{dB/km}$, $\gamma = 0.01$ and $R = 100\,\mu\mathrm{m}$. In this work, the coupling power coefficient of the coupler was fixed with $\kappa = 0.02$. The optical power depends on the nonlinear refractive indices, which range from $n_2 = 2.0$ to $3.4 \times 10^{-17}\,\mathrm{m}^2/\mathrm{W}$. The simulated data of 10,000 iterations, i.e. round trips inside the microring, were shown. We also assume that $\phi_0 = 0$ for simplicity [4]. They have shown that nonlinear effects in the fiber ring resonator could cause problem in the communication system; however, this is useful to implement in the realistic application when the device fabrication is required.

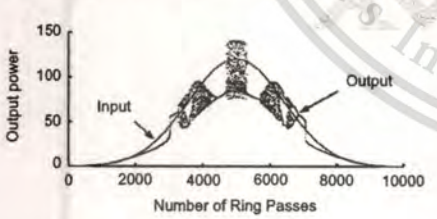

(a)

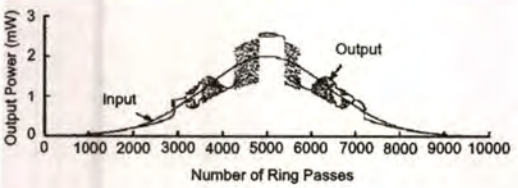

(b)

Fig. 2. (a) Output power for varying number of ring passes, with $\phi_0 = 0$, $n_2 = 3.2 \times 10^{-20}\,\mathrm{m}^2/\mathrm{W}$, $\gamma = 0.1$ and $\kappa = 0.9$; (b) output power for varying number of ring passes, with $\phi_0 = 0$, $n_2 = 2.69 \times 10^{-17}\,\mathrm{m}^2/\mathrm{W}$, $\gamma = 0.01$ and $\kappa = 0.02$.

Fig. 2 shows the curve of output power as a function of the number of ring passes in FORR. The maximum output power resulting from pumping CW envelope is approximately 140 W, and at the beginning the output power is directly proportional to input power. Besides, realizing an optical bifurcation is also achieved when the light passes through the FORR at round trips of 3282 and 3321 times, and optical bifurcation results in optical chaos. Fig. 3 shows the input–output characteristic of the nonlinear FORR with the same parameters as Fig. 2(a). The shape of the hysteresis loop depends on the input pulsewidth. It is found that the hysteresis loop takes place when the input power is in the range of 40.5–46.3 W.

Fig. 4(a)–(c) illustrate the bifurcations of output power and the regions of input power level, which provide the nonlinear effects. The twin bifurcation as shown in Fig. 4(a) can be separated into two bifurcation characteristics with different input powers as Fig. 4(b)–(c). The input power levels at 57.6 and 50 W the bifurcation points of input power levels decreased and increased, respectively. Fig. 5 shows the chaotic characteristics of the nonlinear FORR. We found that the chaos can be realized with input powers in the range of 63–110 W and output is saturated at an input power more than 110 W.

Fig. 6 shows the nonlinear effects on the bifurcation diagram in the input and output power relationship for various nonlinear refractive indices (n_2). The FORR has

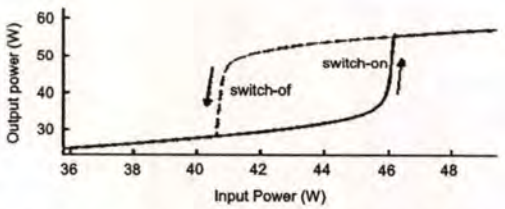

Fig. 3. Optical bistability of the nonlinear FORR. Solid line represents the switch-off power and dash line represents the switch-on power.

Please cite this article as: P.P. Yupapin, et al., Nonlinearity penalties and benefits of light traveling in a fiber optic ring..., Opt. Int. J. Light Electron. Opt. (2007), doi:10.1016/j.ijleo.2007.07.009

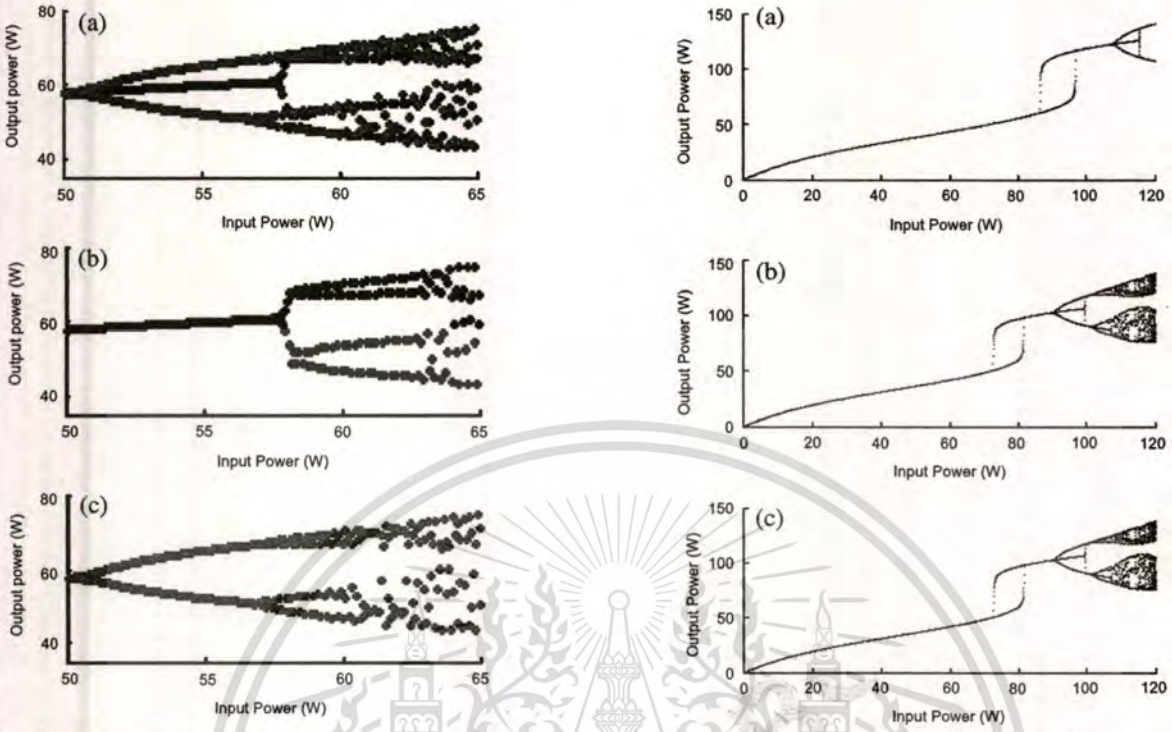

Fig. 4. Bifurcation characteristics of the nonlinear FORR. Here $\kappa = 0.9$, $\phi_0 = 0$ and $n_2 = 3.2 \times 10^{-20}\,m^2/W$. (a) The twin bifurcation of output power, (b) bifurcation with increasing input power and (c) bifurcation with decreasing input power.

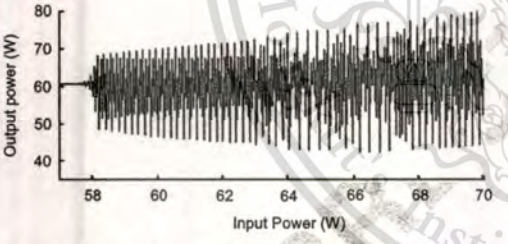

Fig. 5. Chaotic characteristic in the nonlinear FORR.

a circumference $L = 80\,m$ with the coupling coefficients of $\kappa = 0.9$ and the linear phase shift is set to zero. Fig. 6(a) shows that when the nonlinear refractive index is set to $n_2 = 2.2 \times 10^{-20}\,m^2/W$ the region of optical bistability is obtained in the range of 86–97 W and Ikeda unstable effect is in the range of 106–234 W. In addition, we also found that an increase in nonlinear refractive indices can be seen in the regions of optical bistability and Ikeda unstability is in the range of lower input power as shown in Fig. 6(b)–(c).

The next simulated nonlinear effects of the FORR were mainly focussed on the bifurcation diagram in the input and output power relationship by varying linear phase shift (ϕ_0). The other parameters are the same as those used for Fig. 6 and the nonlinear refractive index is set to be $n_2 = 3.2 \times 10^{-20}\,m^2/W$. Here the linear phase

Fig. 6. Bifurcation diagram of the input and output power relation with $\phi_0 = 0$, $\kappa = 0.9$ and $L = 80\,m$ for various nonlinear refractive indices: (a) $n_2 = 2.2 \times 10^{-20}\,m^2/W$, (b) $n_2 = 2.4 \times 10^{-20}\,m^2/W$ and (c) $n_2 = 2.6 \times 10^{-20}\,m^2/W$.

shift of the FORR in Fig. 7 is set at $\phi_0 = 0.25\pi$ rad in (a), $\phi_0 = 0.5\pi$ rad in (b), $\phi_0 = 0.75\pi$ rad in (c) and $\phi_0 = \pi$ rad in (d). The region of the first optical bistability of Fig. 7(a) is found within the range of 46–54.6 W, and at an input power level of approximately 54.6 W the output power is route to bifurcation, while the route to optical chaos occurs at an input power level of 60.7 W and then chaos saturates at an input power level of approximately 120 W. For Fig. 7(b) the region of the first optical bistability is obtained within the range 51.3–63.3 W. The bifurcation points are 59.5 and 63.4 W when the input power levels are decreased and increased, respectively. Bifurcation is the route to optical chaos when the input power level is 64.7 W. However, Fig. 7(c)–(d) does not realize the first optical bistability, but the region of the second optical bistability is found within the range of 57–72.2 and 62.7–81.2 W, respectively.

In application, the penalty benefits of light traveling in the FORR including the nonlinearity of light, optical switching and signal security are described as follows. A four-wave mixing nonlinear type has recently been used to describe a nonlinear effect of light traveling in a fiber optic Sagnac interferometer [12]. They have demonstrated that the standard single-mode fiber incorporating a polarization-maintaining fiber could be used to generate an entangled photon pair. Yupapin and Suchat

Please cite this article as: P.P. Yupapin, et al., Nonlinearity penalties and benefits of light traveling in a fiber optic ring..., Opt. Int. J. Light Electron. Opt. (2007), doi:10.1016/j.ijleo.2007.07.009

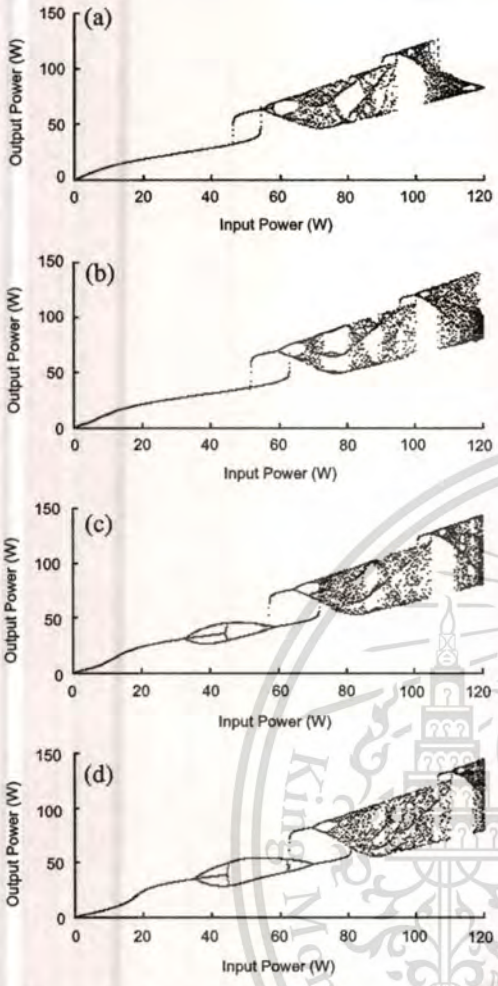

Fig. 7. Bifurcation diagram of the input and output power relation with $n_2 = 3.2 \times 10^{-20}\,\mathrm{m^2/W}$, $\kappa = 0.9$ and $L = 80\,\mathrm{m}$ for various linear phase shifts (a) $\phi_0 = 0.25\pi$, (b) $\phi_0 = 0.5\pi$, (c) $\phi_0 = 0.75\pi$ and (d) $\phi_0 = \pi$.

[13] have recently reported that the nonlinear output light could be obtained after traveling along the FORR. They use weak light instead of the intense light input into the FORR, the nonlinear effect implemented to their setup was the four-wave mixing type. The plot of the simulated data of the nonlinear effects in terms of bifurcation is as shown in Fig. 2. The schematic diagram of four-wave mixing of light in the FORR is as shown in Fig. 8, when the four-wave mixing output, i.e. correlated light, was combined via a polarization combiner and then the entangled photon probability could be detected and observed in terms of the optical output intensity. The other applications can be described using Figs. 3 and 5. Optical switching can be implemented and controlled when the optical input is varied between the specified range. In this case, the optical power ranged between 40 and 46 W, which is extremely high. However, the input power can be reduced when the fiber ring radius is decreased, which can be designed to meet the

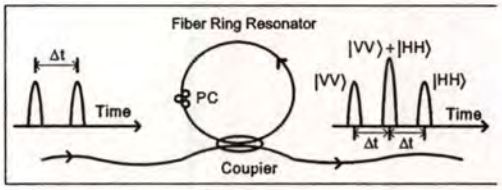

Fig. 8. A schematic diagram of the polarization delay circuit used [13].

specific requirement. The last application is as shown in Fig. 5, the security of the signal can be performed by multiplexing with the chaotic signals (noise), and then the user can make the noise cancellation (chaotic cancellation) before using the required information.

4. Conclusion

In this paper, the nonlinear effects in a FORR including the optical bifurcation, bistability and chaos with the iterative method have been applied to a FORR and presented. Traveling of light in the FORR was analyzed numerically by characterizing the ring radius, nonlinear refractive index and linear phase shift. We have also proposed the use of nonlinearity penalties of light traveling in the FORR in terms of the correlation of light traveling, optical switching and signal security. Results have shown the promising potential application of such proposed penalties as discussed in the various aspects.

Acknowledgments

The authors would like to acknowledge the Department of Applied Physics, Faculty of Science, King Mongkut's Institute of Technology Ladkrabang (KMITL), Thailand, for supporting the laboratory facilities. S. Suchat (Ph.D. candidate) would like to acknowledge the Department of Physics, Faculty of Science and Technology, Thammasat University (TU), Thailand, for some financial support of his study.

References

[1] Y.H. Ja, Multiple bistability in an optical-fiber double-ring resonator utilizing the Kerr effect, IEEE J. Quantum Electron. 30 (1994) 329–333.
[2] J. company, F.J. Praile-Pelaez, M.A. Muriel, Optical bistability and differential amplification in nonlinear fiber resonators, IEEE J. Quantum Electron. 30 (1994) 2578–2588.
[3] K. Ogusu, S. Yamamoto, Nonlinear fiber Fabry–Preot resonator using thermo-optic effect, J. Lightwave Technol. 11 (1993) 1774–1781.

Please cite this article as: P.P. Yupapin, et al., Nonlinearity penalties and benefits of light traveling in a fiber optic ring..., Opt. Int. J. Light Electron. Opt. (2007), doi:10.1016/j.ijleo.2007.07.009

[4] A.L. Steele, S. Lynch, J.E. Hoad, Analysis of optical instabilities and bistability in a nonlinear optical fiber loop mirror with feedback, Opt. Commun. 137 (1997) 136–142.

[5] A.L. Steele, Optical bistability, instabilities and power limiting behaviour from a dual nonlinear optical fiber loop mirror resonator, Opt. Commun. 236 (2004) 209–218.

[6] F.S. Felber, J.H. Marburger, Theory of nonresonant multistable optical devices, Appl. Phys. Lett. 28 (1976) 731–733.

[7] J.H. Marburger, F.S. Felber, Theory of a lossless nonlinear Fabry–Perot interferometer, Phys. Rev. A 17 (1978) 335–342.

[8] T. Bischofberger, Y.R. Shen, Theoretical and experimental study of the dynamic behavior of a nonlinear Fabry–Perot interferometer, Phys. Rev. A 19 (1979) 1169–1176.

[9] K. Ikeda, H. Daido, O. Akimoto, Optical turbulence: chaotic behavior of transmitted light from a ring cavity, Phys. Rev. Lett. 45 (1980) 709–712.

[10] H. Nakatsuka, S. Asaka, H. Itoh, K. Ikeda, M. Matsuoka, Observation of bifurcation to chaos in an all-optical bistable system, Phys. Rev. Lett. 50 (1983) 109–112.

[11] G.P. Agrawal, Nonlinear Fiber Optics, third ed, Academic Press, New York, 2001.

[12] X. Li, P.L. Voss, J.E. Sharping, P. Kumar, Optical-fiber source of polarization-entangled photon pairs in the 1550 nm telecom band, Phys. Rev. Lett. 94 (2005).

[13] P.P. Yupapin, S. Suchat, Entangled photon generation using fiber optic Mach-Zehnder interferometer incorporating the nonlinear effect in a fiber ring resonator, SPIE: J. Nanophotonics (JNP) 1 (2007) 013504. Q3

Please cite this article as: P.P. Yupapin, et al., Nonlinearity penalties and benefits of light traveling in a fiber optic ring..., Opt. Int. J. Light Electron. Opt. (2007), doi:10.1016/j.ijleo.2007.07.009

Far East J. Elec. & Comm.

A QUANTUM CODEC DESIGN VIA AN OPTICAL ADD/DROP MULTIPLEXER IN A FIBER OPTIC NETWORK

P. P. YUPAPIN, P. PHIPHITHIRANKARN and S. SUCHAT

Advanced Research Center for Photonics
Department of Applied Physics
Faculty of Science
King Mongkut's Institute of Technology Ladkrabang
Bangkok 10520, Thailand
e-mail: kypreech@kmitl.ac.th

Abstract

This paper proposes an analysis of quantum code and decode (CODEC) signals via an optical Add/Drop device and fiber optic network, where quantum bits (qubits) can be used to secure the public information. The proposed system design consists of all fiber devices which can be made the practical quantum networks realized. The classical and quantum channel signals can be used as the Add/Drop multiplexing signals via fiber optic link. The Add/Drop multiplexers can be made as a cascade structure to form a larger networks. The compensation of the entangled states in term of timing-walk off from the entangled states in the fiber optic link is analyzed. The optimal entangled states suffer from fiber losses, dispersion and thermal effects are also discussed.

An optical Add/Drop multiplexer has been studied and designed for optical communication applications [4]. However, the perfect information security is extremely required to implement in the communication

2000 Mathematics Subject Classification: **Kindly provide.**

Keywords and phrases: quantum CODEC, quantum networks, quantum key.

Received June 8, 2007

networks. Therefore, the perfect security using quantum encryption has become a good candidate technique to meet this qualification. Since, an optical link has shown the potential of using for long distance quantum communication. Therefore, the use of quantum communication via the optical transmission line, where the confirmation between Alice and Bob can be made. Recently, Yupapin and Suchat [5] have reported the use of weak light to form a nonlinear behavior instead of using strong light pulse in an ordinary single mode fiber, where the four-wave mixing of the two delay light pulses could be performed instead of Kerr effect types. The delayed polarization modes via a ring resonator can be combined with the incoming light pulse, where the entangled photon states are observed and detected. In practice, the remarkably simple design and arrangement of the system are required to make the quantum communication and networks realized. The advantage of such a proposed system is the small scale device could be constructed (fabricated) and used. The applications of the phenomena are such as quantum cryptography, quantum teleportation, quantum key and quantum CODEC that they are popularly studied by Mattle et al. [1], where have demonstrated that atom can be transported by using a classical channel using a Mach-Zehnder Interferometer (MZI), where the single photons which are in linear or circular polarization states can form entanglement pairs, the quantum cryptography by free space has also been reported.

Up to date, the realistic quantum network system has not been implemented in communication line. This letter proposes a technique of quantum communication and networks via the optical Add/Drop multiplexers, where qubits can be performed and used into the public networks. The required information will be retrieved by the individual sender (Alice) and receiver (Bob). However, to implement the system for long distance use, the compensation in delayed time of the entangled states causing the entangled state walk-off is needed. We have also made the analysis and discussion of the signal recovery and compensation of such effects in this proposal.

Firstly, we review the use of an all fiber optic system to generate the entangled photon-pair [5]. When polarized light is input into a MZI, the correspondence between the polarization states and the states obtained

by superposition of the two arm ones can be extended. For example, a polarization coupler that separates the basic vertical and horizontal polarization states corresponds to an optical switch between the short and the long pulses. We assume those horizontally polarized pulses with a temporal separation of Δt. The coherence time of the consecutive pulses is larger than Δt. Then the following time-bin entangled state is created through parametric in MZI, which is expressed as

$$|\Phi\rangle_p = |1, H\rangle_s |1, H\rangle_i + |2, H\rangle_s |2, H\rangle_i. \quad (1)$$

In the expression $|k, H\rangle$, k is the number of time slots (1 or 2), which denotes the state of polarization [horizontal (H) or vertical (V)], and the subscript identifies whether the state is the signal (s) or the idler (i) state. In equation (1), for simplicity, we have omitted an amplitude term that is, common to all product states. We employ the same simplification in subsequent equations in this paper. This two-photon state with H polarization shown by equation (1) is input into the orthogonal polarization delay circuit shown schematically in Figure 1. By the coincidence counts in the second time slot, we can extract the fourth and fifth terms. As a result, we can obtain the following polarization entangled state as

$$|\Phi\rangle = |2, H\rangle_s |2, H\rangle_i + \exp[i(\phi_s + \phi_i)]|2, V\rangle_s |2, V\rangle_i. \quad (2)$$

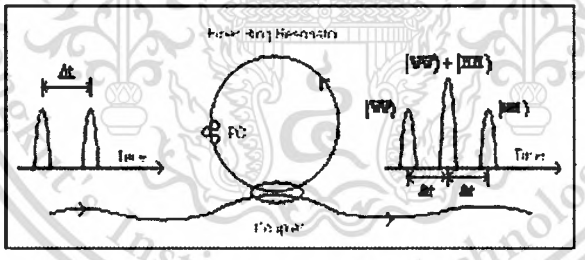

Figure 1. A schematic diagram of the polarization delay circuit that used in the experiment.

To describe how the entangled states transmit via a quantum network, we point out to the four-port device which is configured as an Add/Drop multiplexer (see Figure 2). Two fiber couplers with 50:50

coupling ratios are positioned to tangentially touch opposite sides of an equator of a ring fiber. The four coupling ports are labeled as shown. If a signal containing several channels at the different wavelengths (wavelength division multiplexing) is input at port 1, then their powers transfer to port 2 (network), a ring and drop port (port 3) will occur for any input channel that is, resonant with a fiber ring resonator. There is no resonant channel travel through the upper fiber (port 1) and add port (port 4). Similarly, a channel input at port 4 that is, resonant with a fiber optic ring resonator would be transferred to the upper fiber, and join the other channels at port 2 channel adding and dropping, therefore, this can be realized simultaneously. This is still valid, when the entangled photons are transmitted in to the network. However, in practice, the operation could be suffered by the chromatic dispersion, polarization mode dispersion (PMD) and untargeted nonlinear effects which will be analyzed and discussed.

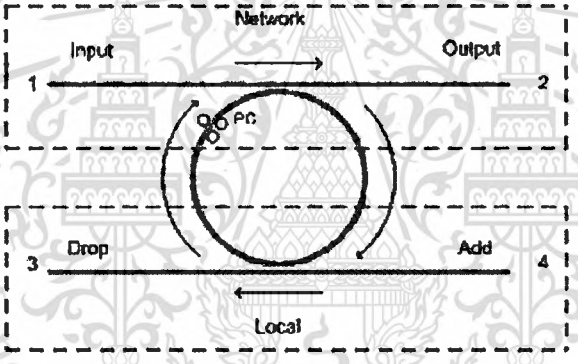

Figure 2. A schematic of a four-port fiber optic device.

When the entangled photon pair which is recognized as the qubits from Figure 1 is launched into a port 4 (add port) in Figure 2, then propagates to the output at port 3 (drop port) and port 2 (throughput port). The output from port 3 is the time delay seen on avalanche photo-detector (confirm states). The entangled photons then transmit into the transmission line (port 2), while the confirmed states are seen on a photo-detector at port 3 (Alice). The entangled states with wavelength multiplexing are distributed within the networks, the projection of the

specific wavelengths can be recovered by Bob at the required drop ports. Generally, the classical and quantum channel signals can input into the network via the Add/Drop multiplexers then into the transmission lines. Further, the optical Add/Drop multiplexers can be designed as a cascade to form a larger networks. The specific quantum protocol is also available to implement in this purposed system. The incoming multi-wavelength signals at the input port, where all wavelength channels are routed into the throughput port except the required drop wavelength, which is routed to the drop port, therefore, drop port is actually required the wavelength tunable filters to obtain the precisely receive the request information.

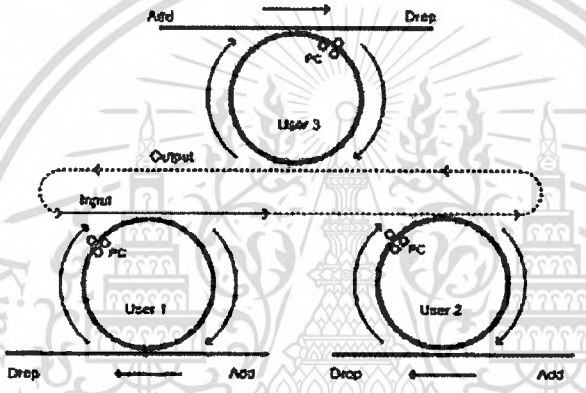

Figure 3. A schematic of a four-port device in a quantum network.

After the signal that is processed by the drop port, then the same carrier wavelength with different information can be added simultaneously into the ring and network via the add port. The schematic of the optical Add/Drop and network is as shown in Figure 3. Wavelengths tunable filters are essential required in each of the Add/Drop ports. In practice, the simple design and arrangement of the system are required to make the quantum communication and networks realized. In applications, the idea of dense coding with dense input or dense wavelength multiplexing (DWDM) with wide range of bandwidth applications can be implemented, where the communication data without any cheating between users in the public link is plausible.

When the quantum states with a temporal delay Δt is launched into User 1 at the add port, which can be written as

$$|\psi\rangle = \alpha|H\rangle_{\Delta t} + \beta|V\rangle_{\Delta t}. \tag{3}$$

The photons in the H and V polarization states are transmitted through the four-port device, where the channel short and long fiber lengths are given, respectively. Here, a length of an ordinary single mode fiber can be employed to transmit the quantum channels. For simplicity, we also use the polarization control fibers (PC) included in the system. In this case, the polarization rotations of the photons in each channel does not occur, but unknown phase shifts ϕ_H and ϕ_V are added to the photons in each channel independently due to the fluctuations of light in the optical path lengths. We assume that the interval Δt between the signal and idler photons much shorter than the correlation time of the fluctuations, so that the phase shifts are considered to be correlated such that $\phi_H(t) = \phi_H(t + \Delta t) = \phi_H$ and $\phi_V(t) = \phi_V(t + \Delta t) = \phi_V$. The photons in both modes, long and short arms, are then mixed together, and the received states at drop port after circulation in a fiber ring resonator, which can be written as

$$\frac{1}{\sqrt{2}}[\alpha e^{2i\phi_H}|H\rangle|H\rangle_{\Delta t} + \beta e^{2i\phi_V}|V\rangle_{\tau}|V\rangle_{\Delta t+\tau} + e^{i(\phi_H+\phi_V)}(\alpha|V\rangle_{\tau}|H\rangle_{\Delta t} + \beta|H\rangle|V\rangle_{\Delta t+\tau})]. \tag{4}$$

Here the optical path lengths of short and long may differ, which is indicated by the temporal delay τ. To confirm the entangled states relationship between drop port and fiber ring resonator, a PC is adjusted before the powers transferring into a network via an optical switching (port 2). Similarly, the other users can generate the entangled states (qubits) with a specific wavelength into add port. The entangled states are confirmed before entering into the networks. The optical filters are employed to obtain the specific wavelengths (decode) at the users. The larger networks are also available with the same analysis, where the optical filters are required to retrieve the qubits.

Due to the birefringence of the fiber, a transversal walk-off the extraordinary beam and longitudinal walk-off between the ordinary and

extraordinary beam will occur. The transversal walk-off produces a shift between the ordinary and extraordinary while the longitudinal walk-off introduces a time delay between horizontally and vertically polarized photons. The amount of the walk-off depends on the location, where the photon-pairs are created within the fiber. This position is completely random due to the coherent nature of light in fiber optic. To compensate the longitudinal timing-walk off effect, a polarization controller is recommended to ensure that polarization rotation is the same on both photons from the entangled pair. Additionally, the compensator fiber (dispersion shift fiber, DFB) is used to change the relative phase ϕ of the states of the polarized light. Because of their birefringence, the tilting of the compensator allows to apply a phase shift to the state [3]

$$|\psi\rangle_{12} = \frac{1}{\sqrt{2}}(|H\rangle_1 \otimes |V\rangle_2 + e^{i\phi}|V\rangle_1 \otimes |H\rangle_2). \tag{5}$$

In our case, we want to produce the $|\psi^-\rangle$ state, which can be obtained by setting the phase $\phi = \pi$. Thus, linear polarized light passing through an optical fiber can be converted to any linear combination of linear and circular polarization. This polarization rotation varies with stress and strain imposed on the fiber by bending the fibers or by temperature changes. Moving or even touching the fiber changes the polarization rotation effect unpredictably. To preserve the state of the created photon pair, the polarization rotation of the optical fibers had to be compensated. For this letter, we propose the system based on all fiber optic scheme, therefore, the used of fiber based polarization control is arranged.

In the maximally entangled pure state our setup supposed to produce is the anti-symmetric singlet

$$|\psi^-\rangle_{12} = \frac{1}{\sqrt{2}}(|H\rangle_1 \otimes |V\rangle_2 - |V\rangle_1 \otimes |H\rangle_2). \tag{6}$$

However, in practice, it is never possible to create a pure state; instead, a mixed state is produced. For the further treatment of the quality of our source, we need to make an assumption of how this state looks like. For that purpose, polarizer controllers are placed into the coupling path of both photons, the photons collected into the optical fibers are detected in entangled photons detection modules. By matching the time of arrival of

the two photons at their corresponding detection modules, it is possible to determine a joint detection event, also called *coincidence event* and thus, to establish polarization correlation between entangled photon-pairs.

To implement such a scheme incorporating in an optical communication networks, the effects on fiber optic properties in network such as spectrum noise, signal dispersion, fiber losses, and timing walk-off on the entangled states are required to make the system validate. When light propagates in fiber ring resonator, where the ring radius could be ranged from micrometer to few kilometers, the problem is the signal spacing among the propagating signals, which is well described by Saeung and Yupapin [5]. In case of multi-photons, the signal spacing regions known as the *signal free spectral ranges* (FSR) are required to design to meet the specific purpose. This parameter can be caused the intermodulation noises of the signals in the ring resonator and network link.

In conclusion, we proposed the technique of quantum CODEC signals, which can be used in the optical networks. This can be performed by using the remarkably simple arrangement of the entangled photons generation source and the optical Add/Drop multiplexer. When the projection devices are applied (Bob), and the state is confirmed (Alice), the quantum CODEC signals could be seen by the users (Alice and Bob). A top security information using the quantum CODEC technique based on quantum cryptography by light, i.e., qubits, has been proposed and discussed. The compensation of the timing-walk off on the entangled states is analyzed and also discussed.

Acknowledgements

The authors would like to thank the Department of Applied Physics, Faculty of Science, King Mongkut's Institute of Technology Ladkrabang (KMITL), Thailand, for supporting the laboratory facilities. S. Suchat (Ph.D. candidate) thanks the Department of Physics, Faculty of Science and Technology, Thammasat University (TU), Thailand, for some financial support to his study.

References

[1] K. Mattle, H. Weinfurter, P. G. Kwiat and A. Zeilinger, Phys. Rev. Lett. 76 (1996), 4656.

[2] P. Saeung and P. P. Yupapin, Optical Engineering, 2007. **Kindly provide publisher's name.**

[3] P. Trojek, Ch. Schmid, M. Bourennane and H. Weinfurter, Opt. Express 12 (2004), 76.

[4] P. P. Yupapin, P. Saeung and C. Li, Opt. Comm. 272 (2007), 81.

[5] P. P. Yupapin and S. Suchat, J. Nanophotonics (JNP) 1 (2007), 013504.

■

BIOGRAPHY

NAME	MR. SUEBTARKUL SUCHAT
DATE OF BIRTH	6 DECEMBER 1967
PLACE OF BIRTH	CHONBURI
INSTITUTION ATTENED	Ramkhamhang University, 1988-1992 Bachelor of Science (Physics) King Mongkut's Institute of Technology Ladkrabang, 1995-1999 Master of Science (Applied Physics) King Mongkut's Institute of Technology Ladkrabang, 2000-2007 Doctor of Philosophy (Applied Physics)
POSITION & OFFICE	1994-Present, Dept. of Physics, Faculty of Science & technology, Thammasat University, Prathumthani, Thailand.